Synthetic biological studies on production of methanol from natural resource-derived carbon compounds

Tomoyuki Takeya

2021

Contents

Introduction

Methanol is a useful feedstock for various chemicals and value-added products, e.g. plastic materials and pharmaceuticals. In bioindustry, methanol is a low-priced carbon source for methylotrophic microorganisms (methylotrophs) which produce recombinant protein, pyrroloquinoline quinone and so on (Schrader et al. 2009). In addition, methanol has an excellent property as a fuel or an energy storage medium (Olah et al. 2009). Methanol is currently produced from syngas (CO/H_2), which is derived from natural gas, biomass or coal. Moreover, production of methanol by chemical recycling of CO_2 has been attempted. Taken together, methanol is a versatile compound to which a huge range of natural resources can be converted, and for this reason, the methanol economy, an economy where methanol plays a central role as a sustainable carbon and energy resource, has been proposed by a Nobel Laureate in Chemistry Olah et al. (Olah et al. 2009).

In nature, methanol is a part of the carbon cycle, produced by diverse kinds of methanol-producing enzyme, such as pectin methylesterase (PME) and methane monooxygenases (MMOs). PME is possessed by organisms from multiple kingdoms (Kohli et al. 2015), while MMOs are produced by methanotrophic bacteria (methanotrophs), which can grow on methane as a sole source of carbon and energy (Chan and Lee 2019; Ross and Rosenzweig 2017; Sirajuddin and Rosenzweig 2015). These enzymes are expected to be used for methanol production from pectin (in plant biomass) and from methane (a main component of natural gas), respectively. On the other hand, methanol is consumed by methylotrophs through various types of one-carbon metabolism (C1 metabolism). Interestingly, some of the enzymes involved in C1 metabolism can catalyze reverse reactions in the direction from biomass constituents to methanol (Arfman et al. 1989; Orita et al. 2006). These methanol-producing enzymatic reactions can be adopted for microbial production of methanol from

natural resource-derived carbon compounds.

Recently, microbial production of chemicals has been largely facilitated by synthetic biology approaches. For example, productivity of the target compound within single microbial cells can be visualized with genetically encoded biosensor, such as a fluorescent protein gene under the control of the target compound-inducible gene promoter, enabling remarkably fast and mass screening of the "high producer" in combination with fluorescence-activated cell sorting (FACS) (Jha et al. 2014; Mustafi et al. 2012). In addition, synthetic metabolic pathways can be designed and implemented in nonnative microbial hosts to produce the target compound through multistep enzymatic reactions (DeLoache et al. 2015).

In this thesis, I describe synthetic biological studies on production of methanol from natural resource-derived carbon compounds. I developed a yeast single cell-based biosensing technology for methanol produced by enzyme reactions, and applied it for single-cell visualization of the methanol-producing enzyme activities, towards the high-throughput screening of the "high producer". I also describe construction of a synthetic methanol-producing metabolic pathway in a non-methylotrophic bacterial cell using the reverse reactions catalyzed by C1 metabolic enzymes.

In Chapter I, I conducted single-cell analyses of the methylotrophic yeast *Komagataella phaffii* (recently reclassified from *Pichia pastoris*) to develop a biosensor for the detection of methanol produced by heterologous enzymes. In this biosensor, methanol and its subsequent metabolism induce expression of a gene encoding a fluorescent protein that was placed under the control of methanol-inducible promoter. Using quantitative analyses of fluorescence microscopy images, a methanol-inducible promoter and a host strain were selected, and preculture and assay conditions were optimized to improve the methanol detection limit. Flow cytometric analysis of the distribution and geometric mean of cellular fluorescence intensity against various concentrations of methanol revealed a detection limit of 2.5 μM.

In Chapter II, the developed yeast methanol sensor was applied to visualize the activity of methanol-producing enzyme activity. In Section I, I conducted heterologous expression of PME using the methanol sensor cell as a host. The cellular fluorescence intensity was proportional to the copy number of the PME expression cassette, the protein level, and the enzyme activity. These results proved the concept of the use of the methanol sensor for visualization of methanol-producing enzyme activity at a single-cell level, which enables high-throughput screening of single cells harboring high methanol-producing activity, and thereby, of engineered enzymes with high activity and/or stability.

In section II, I visualized methane oxidation activity of propane-utilizing bacterium *Mycolicibacterium* sp. TY-6 cells (Kotani et al. 2006) by co-culture with methanol sensor cells in the presence of methane. In this co-culture, the methanol sensor cells gave increase of fluorescence intensity depending on methane and cell density of *Mycolicibacterium* sp. TY-6. This result successfully establishes the use of the methanol sensor for detection of biological methane oxidation activity and the co-culture for one-pot synthesis of a heterologous protein (fluorescent protein) with methane. I next attempted to express methane-oxidizing biocatalysts (MOBs) including MMOs in the methanol sensor cells, but could not detect consistent activities. Non-enzymatic oxidation of methane, which may interfere with biological methane oxidation activity assay, turned out to occur in the presence of a quinol compound contained in the assay or hydrogen peroxide (H_2O_2), under physiological conditions, explaining the controversy in the present and previous studies on biological methane oxidation that used the quinol compound.

In Chapter III, I constructed a reversed methylotrophic pathway that produces methanol from fructose 6-phosphate (F6P), which can be supplied by catabolism of biomass-derived sugars including glucose, by a synthetic biology approach. Using *Escherichia coli* as an expression host, I heterologously expressed genes encoding methanol utilization enzymes from methylotrophic bacteria, i.e., the NAD^+-dependent methanol dehydrogenase (MDH) from

Bacillus methanolicus S1 (reclassified from *B. brevis* S1) (Arfman et al. 1992; Yurimoto et al. 2002) and an artificial fusion enzyme of 3-hexulose-6-phosphate synthase and 6-phospho-3-hexuloisomerase from *Mycobacterium gastri* MB19 (HPS-PHI) (Orita et al. 2007). I confirmed that these enzymes can catalyze reverse reactions of methanol oxidation and formaldehyde fixation. The engineered *E. coli* strain co-expressing MDH and HPS-PHI genes produced methanol in resting cell reactions not only from F6P but also from glucose. I successfully conferred reversed methylotrophy to *E. coli* and my results provide a proof-of-concept for biological methanol production from biomass-derived sugar compounds.

Chapter I
Development of methanol-biosensing technology by yeast single-cell analyses

Introduction

In bioconversion processes using recombinant enzymes in microbial cells, the productivity of the target compound depends largely on the activity and stability of the relevant enzyme being produced. To be successful, it is critical to develop a high-throughput system for screening microbial cells with high enzyme activity and/or stability. Recently, approaches using single-cell analyses have enabled us to conduct such high-throughput screening at a single-cell level. If a biosensor that produces fluorescence in response to the reaction product of the recombinant enzyme is created, cells having higher enzyme activity can be selected at a single-cell level in a high-throughput manner, e.g. via FACS technology (DeLoache et al. 2015; Ho et al. 2018; Jha et al. 2014; Michener et al. 2012; Mustafi et al. 2012).

To exploit the potential of methanol-producing enzymes for bioconversion processes, a sensitive method to evaluate their activities at a single-cell level should be established. So far, several biosensors for methanol detection have been reported with microbial cells or enzymes immobilized on an oxygen electrode (Guilbault et al. 1983; Wen et al. 2014). However, these biosensors cannot be used for the detection of methanol endogeneously produced by recombinant enzymes. We and others previously described biosensors for methanol detection based on the expression of a fluorescent protein gene under the control of a methanol-inducible promoter (Abanda-Nkpwatt et al. 2006; Kawaguchi et al. 2011). In these fluorescent biosensors, the fluorescence intensity of single cells was analyzed with fluorescence microscopy. However,

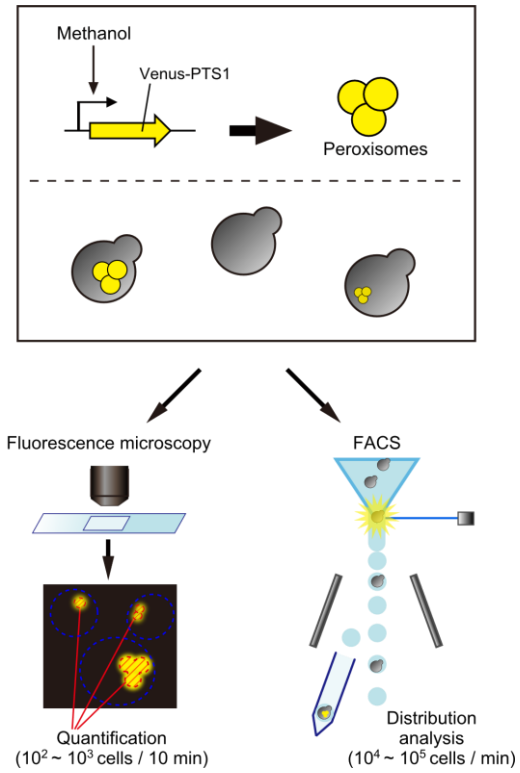

Fig. 1-1 Schematic illustration of the *K. phaffii* single-cell methanol sensor. The fluorescent protein Venus tagged with peroxisome targeting signal 1 (Venus-PTS1) is expressed under control of a methanol-inducible promoter. These cells show methanol-dependent fluorescence in peroxisomes. Fluorescence microscopy enables visual assessment of the cellular response, and the cellular fluorescence intensity can be determined by image analysis (10^2~10^3 cells per 10 min). FACS analysis enables high-throughput analysis and sorting of single cells (10^4~10^5 cells/min).

the detection limit needed to be improved to detect enzymatically produced levels of methanol for application to high-throughput analysis such as FACS.

In this chapter, I developed a single-cell biosensor for methanol detection with the methylotrophic yeast *K. phaffii*, which has been widely used as a host for heterologous protein production (Ahmad et al. 2014; Gellissen 2000). Methylotrophic yeasts, capable of utilizing methanol as the sole carbon and energy source, have methanol-sensing machinery to respond to widely fluctuating methanol concentrations in nature as well as in laboratory culture

(Kawaguchi et al. 2011; Ohsawa et al. 2017). Fig. 1-1 shows the design of the new methanol biosensor. Expression of a gene encoding a fluorescent protein under the control of a methanol-inducible promoter is induced by methanol in a dose-dependent manner and completely repressed by the presence of glucose. Selection of the promoter, optimization of sensing conditions, and analysis of the distribution of cellular fluorescence intensity by FACS improved the limit of detection for methanol to the micromolar range.

Materials and methods

Strains and media

The yeast strains used in this study are listed in Table 1-1. *K. phaffii* cells were grown at 28 °C on glucose medium (1% yeast extract, 2% peptone, 2% glucose). The assay media for the detection of methanol (methanol medium) contained 0.67% yeast nitrogen base without amino acids and 0–2.5×10^5 μM methanol. All of the components in these media other than carbon sources were purchased from Becton Dickinson (Franklin Lakes, NJ). Cell growth was monitored by the optical density at 610 nm (OD_{610}).

Table 1-1 Yeast strains used in this study

Strain	Genotype	Description	Source or reference
PPY12	*his4 arg4*	Wild type	Gould et al. (1992)
PMT1101	PPY12 *his4*::pAOX1V (P_{AOX1}-Venus-PTS1 *HIS4*)	Auxotrophic methanol sensor candidate strain	This study
PMT1301	PPY12 *his4*::pDAS2V (P_{DAS2}-Venus-PTS1 *HIS4*)	Auxotrophic methanol sensor strain	This study
PMT1102	PMT1101 *arg4*::pNT204 (*ARG4*)	Non-auxotrophic methanol sensor candidate strain	This study
PMT1302	PMT1301 *arg4*::pNT204 (*ARG4*)	Non-auxotrophic methanol sensor strain	This study
KM71	*his4 arg4 aox1*Δ::*ScARG4*	*aox1*Δ	Invitrogen
PMT1401	KM71 *his4*::pDAS2V (P_{DAS2}-Venus-PTS1 *HIS4*)	Methanol sensor strain with *aox1*Δ background	This study

Table 1-2 Oligonucleotide primers used in this study

Primer	Sequence (5'-3')	Purpose
Venus-fw-Kpn1	TCGGTACCAAAATGGTGAGCAAGGGCGAGG	Amplification of Venus gene fused with PTS1 at the C-terminus for construction of pAOX1V
Venus-rv-SKL-BamH1	AGTGGATCCTCACAACTTAGACTTGTACAGCTCGTCCATG	
PDAS(0834)-fw-Aat2	CCACCTGACGTCAATAAAAAAACGTTATAGAAAGAAATTGGACT	Amplification of 1.0-kb upstream region of the *DAS2* gene for construction of pDAS2V
PDAS(0834)-rv-Sac1	ACCGAGCTCTTTGTTCGATTATTCTCCAGATAAAATCAAC	

Plasmid construction and transformation

The oligonucleotide primers used in this study are listed in Table 1-2. The plasmids used in this study are listed in Table 1-3. pAOX1V was obtained by inserting the 0.7-kb Venus gene (Nagai et al. 2002) fused to the peroxisome targeting signal 1 (PTS1) sequence (Ser-Lys-Leu) into the KpnI/BamHI sites of pIB4 (Sears et al. 1998). pDAS2V was constructed by removing the promoter region of pAOX1V between the AatII/SacI sites, where the 1.0-kb upstream region of

Table 1-3 Plasmids used in this study

Plasmid	Description	Source or reference
pIB4	*HIS4*; P_{AOX1}-based expression vector	Sears et al. (1998)
pAOX1V	Venus-PTS1 inserted into KpnI/BamHI sites of pIB4	This study
pDAS2V	1.0-kb upstream region of the *DAS2* gene inserted into AatII/SacI sites of pAOX1V	This study
pNT204	*ARG4*	Tamura et al. (2010)

the *DAS2* gene was inserted. pAOX1V and pDAS2V were linearized at the StuI site, and pNT204 was linearized at the SacI site, for transformation. *K. phaffii* cells were transformed by electroporation as described previously (Wu and Letchworth 2004).

Fluorescence microscopy and image analysis

Non-auxotrophic strains were derived by introduction of the corresponding auxotrophic gene, and used for image and FACS analysis. Cells were observed with a motorized inverted microscope (IX81; Olympus, Tokyo, Japan) equipped with an Uplan-Apochromat 100x/1.35 NA oil iris objective lens. Venus signal was acquired using 500AF20, 455DRLP and 535AF30 filter sets (Omega Optics, Austin, TX). Image data were captured with a charge-coupled device camera DP30BW (Olympus) at a fixed exposure time of 100 msec. For each sample, one field with at least 100 cells was captured. Data were acquired and analyzed by using MetaMorph software version 7.0 (Molecular Devices, San Jose, CA) and saved as 16-bit TIFF files. Quantification of fluorescence intensity was conducted with ImageJ software version 1.51n (https://imagej.nih.gov/ij/) as follows. The threshold was set from 145 to 4095 to measure the fluorescence intensity of pixels covering peroxisomes. Fluorescence intensity of the pixels within the set threshold was averaged to represent the cellular fluorescence intensity of the image (expressed as arbitrary units, a.u.). Three independent experiments starting from distinct single colonies were conducted.

Flow cytometry

Cells were resuspended in ice-cold phosphate buffered saline (PBS) buffer and kept on ice. Flow cytometry was performed using FACSAria IIIu (Becton Dickinson). Fluorescent channel and light scatter were set at log gain. The forward scatter (FSC) was set at a photomultiplier tube (PMT) voltage of 250 with a threshold of 2000. The side scatter (SSC) PMT voltage was

set at 250. Venus fluorescence was excited with a 488 nm laser and the emission at 530/30 nm was detected at a PMT voltage of 700 or 900. At least 30,000 cells were analyzed per sample. Cells were gated for forward and side scatter to select single cells as shown in Fig. 1-4a-c. Since Venus fluorescence intensity (Venus-A) was proportional to forward scatter (FSC-A), which reflects cell size (Fig. 1-4d), Venus-A normalized to FSC-A (Venus-A/FSC-A) with 25% scaling was used to represent the fluorescence intensity of each cell. FACSDiva 8 software (Becton Dickinson) was used for data acquisition and creation of scatter plots. Bioconductor (www.bioconductor.org) in the open-source statistical platform R (www.r-project.org) was used for processing of FCS data, followed by preparation of histograms.

Results

Construction of the *K. phaffii* methanol sensor strain and optimization of assay conditions

K. phaffii strains expressing the yellow fluorescent protein Venus (Nagai et al. 2002) tagged with peroxisome targeting signal 1 (PTS1) under the control of strong and methanol-inducible promoters, P_{DAS2} (dihydroxyacetone synthase gene) and P_{AOX1} (alcohol oxidase gene) (Liang et al. 2012; Stewart et al. 2001; Vogl et al. 2016) were constructed. Since peroxisome proliferation is coupled with methanol-induced expression of peroxisomal enzymes, Venus was targeted to peroxisomes, which could give an intense punctate fluorescence signal distinguishable from the cytosolic background.

To repress the expression of the reporter Venus-PTS1 protein, cells were first grown on glucose medium, harvested at mid- or late-exponential phase (Fig. 1-2), and the effect of the growth phase on expression was examined. Harvested cells were transferred into medium containing various concentrations of methanol (0–2.5×10^3 μM) (methanol medium). After 4 h of incubation, at least 100 cells from each sample were observed in one field under a fluorescence microscope and the cellular fluorescence intensity was quantified using ImageJ software (“Materials and methods” section). The detection limit of the strain is defined as the

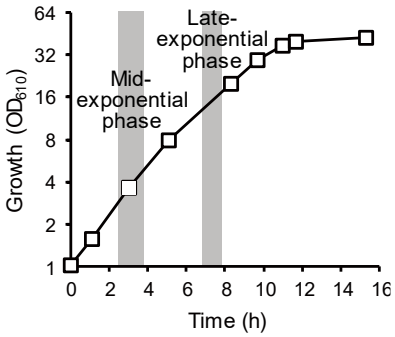

Fig. 1-2 Typical growth curve of the *K. phaffii* methanol sensor strain on glucose medium.

lowest concentration of methanol showing cellular fluorescence intensity statistically higher than that without methanol.

When the mid-exponential phase cells grown in glucose medium were used for analysis, cellular fluorescence intensity with P_{DAS2} at 250 μM methanol, but not 2.5 or 25 μM, was significantly higher than that without methanol (Fig. 1-3a (left), $p < 0.05$). When P_{AOX1} was used, the cellular fluorescence intensity at 2.5×10^3 μM methanol, but not 2.5–2.5×10^2 μM, was significantly higher than that without methanol (Fig. 1-3a (right), $p < 0.01$). Therefore, the detection limit of the strain using P_{DAS2} (2.5×10^2 μM) was lower than that of the strain using P_{AOX1} (2.5×10^3 μM).

When late-exponential phase cells were used for analysis, cellular fluorescence intensity with P_{DAS2} at 25 μM methanol was significantly higher than that without methanol (Fig. 1-3b (left), $p < 0.01$) and increased as the concentration of methanol increased up to 2.5×10^3 μM (Fig. 1-3b (left) and c). Thus, the detection limit and dose-dependency of methanol was improved by using late-exponential phase cells. A similar experiment using the strain with P_{AOX1} resulted in a detection limit of 2.5×10^2 μM, confirming that P_{DAS2} shows a lower detection limit under these conditions as in the case using mid-exponential phase cells (Fig. 1-3b, right). Accordingly, the strain expressing Venus-PTS1 under the control of P_{DAS2} was designated as the methanol sensor strain, and late-exponential phase cells were used in subsequent experiments.

I also tested a methanol sensor strain with an *aox1*Δ background with the expectation that disruption of the alcohol oxidase gene would diminish methanol consumption and result in an improved detection limit. However, the detection limit of this strain was 2.5×10^3 μM (Fig. 1-3d, $p < 0.05$). This observation is consistent with results of our previous study with another methylotrophic yeast, *Candida boidinii,* in which deletion of the alcohol oxidase gene (*AOD1*) resulted in a decrease in *AOD1* promoter activity (Sakai et al. 1999). Therefore, not only methanol itself but also its metabolism, yielding metabolites and energy, are considered

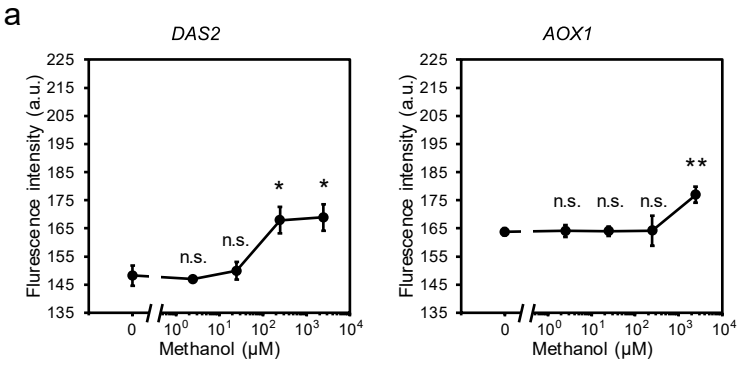
a
DAS2
AOX1
Flurescence intensity (a.u.)
Methanol (μM)
n.s.
*
**

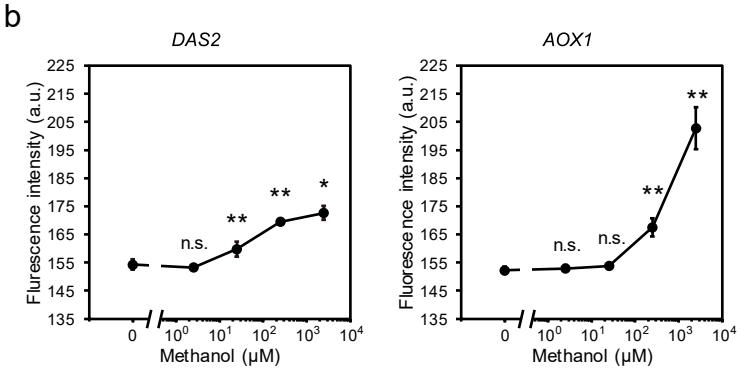
b
DAS2
AOX1
Flurescence intensity (a.u.)
Methanol (μM)
n.s.
*
**

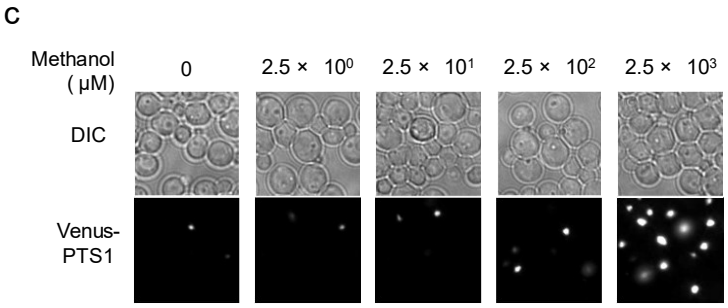
c
Methanol (μM)
0
2.5 × 10^0
2.5 × 10^1
2.5 × 10^2
2.5 × 10^3
DIC
Venus-PTS1

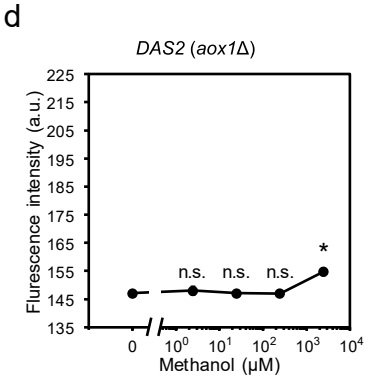
d
DAS2 (aox1Δ)
Flurescence intensity (a.u.)
Methanol (μM)
n.s.
*

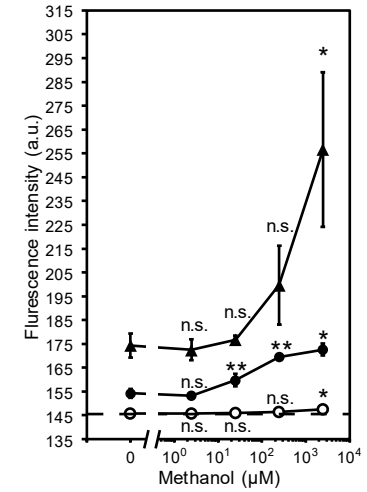
e
Flurescence intensity (a.u.)
Methanol (μM)
n.s.
*
**

Fig. 1-3 Development of a *K. phaffii* single-cell methanol sensor using fluorescence microscopy. **a** Comparison of the dose-response of two methanol-inducible promoters, P_{DAS2} and P_{AOX1}, using cells precultured on glucose medium to mid-exponential phase (Fig. 1-2) and transferred to medium containing various concentrations of methanol. Cells were observed after 4 h of incubation. **b** Similar analyses using cells precultured on glucose medium to late-exponential phase (Fig. 1-2). **c** Fluorescent images of methanol sensor cells using P_{DAS2} transferred from late-exponential phase preculture on glucose medium to the indicated methanol medium, together with differential interference contrast (DIC) microscopic images. **d** Influence of *AOX1* gene disruption on the dose-response of methanol sensor cells. Cells were precultured and analyzed as in Fig. 1-3b. **e** Time-course analysis of the dose-response. Cells were precultured and transferred into methanol medium as in Fig. 1-3b. Cells sampled at 2 h (open circles), and 6 h (closed triangles) during incubation in methanol medium were analyzed and compared with 4 h (closed circles) in Fig. 1-3b. Dashed line indicates the fluorescence intensity level at 0 h without methanol (145.62 ± 0.05). Fluorescence intensity data are expressed in arbitrary units (a.u.) and represent means ± standard deviations of three independent experiments. Each experiment consisted of a glucose culture starting from a distinct single colony followed by transfer to methanol medium, resulting in one sample for each concentration. For each sample, the cellular fluorescence intensity was calculated from the image data of one field containing at least 100 cells. Statistical significance against the data at 0 μM methanol was calculated by two-tailed paired *t* test (n.s., $p > 0.05$; *, $p < 0.05$; **, $p < 0.01$).

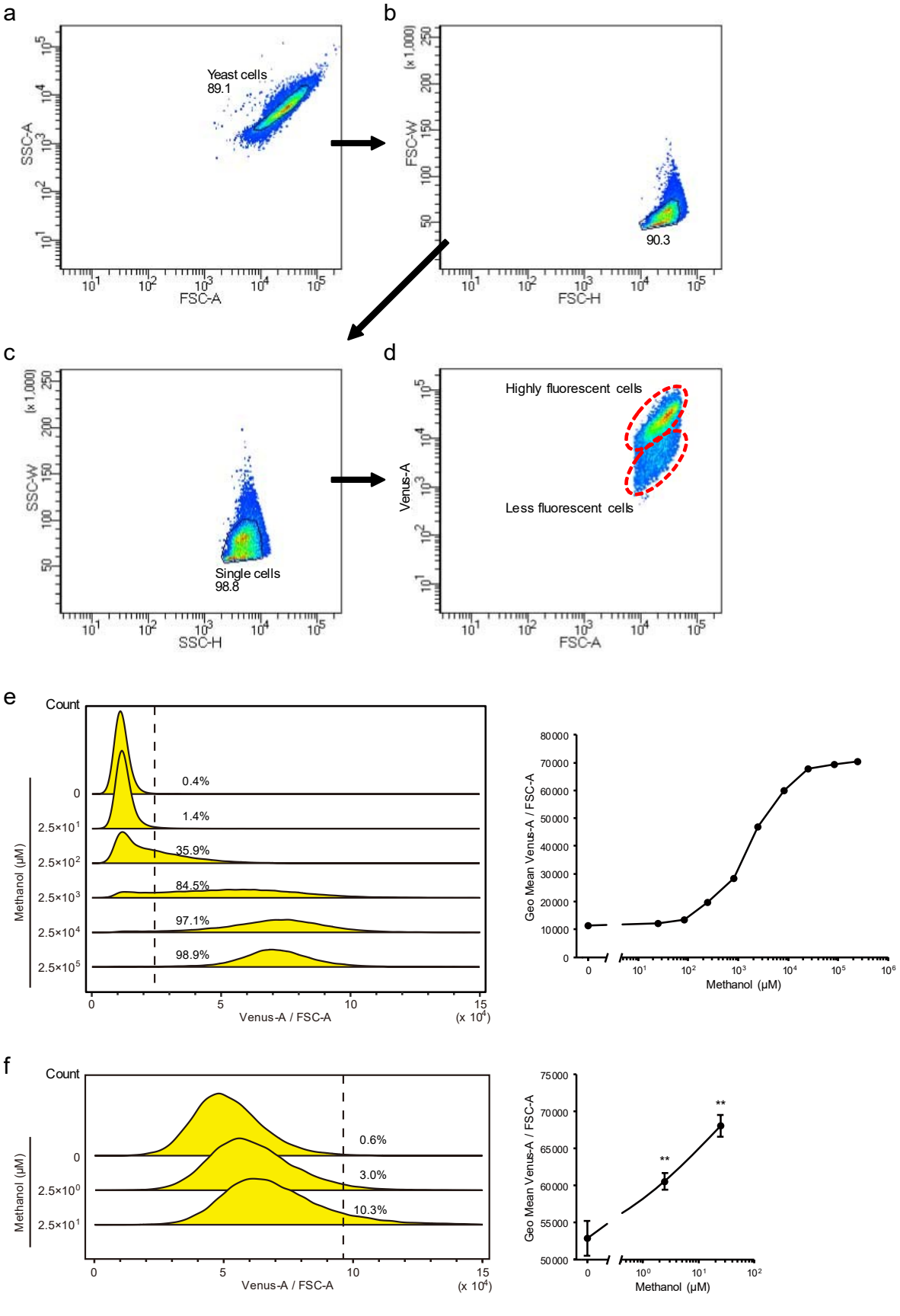
a
Yeast cells
89.1
SSC-A
FSC-A
b
FSC-W
FSC-H
90.3
c
SSC-W
SSC-H
Single cells
98.8
d
Highly fluorescent cells
Less fluorescent cells
Venus-A
FSC-A
e
Count
Methanol (μM)
0
2.5×10^1
2.5×10^2
2.5×10^3
2.5×10^4
2.5×10^5
0.4%
1.4%
35.9%
84.5%
97.1%
98.9%
Venus-A / FSC-A
(x 10^4)
Geo Mean Venus-A / FSC-A
Methanol (μM)
f
Count
Methanol (μM)
0
2.5×10^0
2.5×10^1
0.6%
3.0%
10.3%
Venus-A / FSC-A
(x 10^4)
Geo Mean Venus-A / FSC-A
**
**
Methanol (μM)

Fig. 1-4 Distribution and dose-response of the cellular fluorescence intensity of methanol sensor cells, revealed by FACS analyses. Cells were precultured on glucose medium to late-exponential phase and transferred to methanol medium and analyzed after 4 h of incubation. Single cells were selected using the gates from **a** to **c** in order. **a** Yeast cells were selected on the basis of the forward scatter area (FSC-A) and the side scatter area (SSC-A). **b** First selection of single cells on the basis of the forward scatter height (FSC-H) and the width (FSC-W). **c** Second selection of single cells on the basis of the side scatter height (SSC-H) and width (SSC-W). **d** Plot of the Venus fluorescence area (Venus-A), detected at a PMT voltage of 700, against FSC-A of the single cells. The Venus-A of highly fluorescent cells and less fluorescent cells were both proportional to each FSC-A. Hereafter the Venus fluorescence normalized to the forward scatter (Venus-A/FSC-A value) was used to represent the fluorescence intensity of the single cells. **e, f** Distribution and geometric mean of the Venus-A/FSC-A values at various concentrations of methanol measured at a Venus PMT voltage of 700 (**e**) or 900 (**f**). At least 30,000 cells were measured to generate each histogram and calculate each geometric mean. The maximum level of the Venus-A/FSC-A value without methanol is defined as the value indicated by dashed lines on the histograms. Percentages of cells with Venus-A/FSC-A values above the maximum level without methanol are indicated on the histograms. For **f**, the histograms represent typical data from three independent experiments starting from three distinct single colonies, followed by transfer to methanol medium in triplicate. Data from triplicates were averaged for each independent experiment, and shown on the plot. Error bars represent means ± standard deviations of three independent experiments. Statistical significance against the data at 0 μM methanol was calculated by two-tailed paired *t* test (**, $p < 0.01$).

to be necessary for full induction of Venus-PTS1 under the control of P_{DAS2}. Accordingly, the wild-type methanol sensor strain, rather than the *aox1*Δ strain, was used in the following analyses.

Finally, I conducted a time-course analysis of the methanol sensor cells to optimize the incubation time prior to observation. The methanol sensor cells were incubated in methanol medium and observed at 2-h intervals for 6 h. The cellular fluorescence intensity with 0–2.5 × 10^2 μM methanol at 2 h was almost the same as that at 0 h, while the cellular fluorescence intensity at 2.5 x 10^3 μM methanol was significantly higher than that without methanol (Fig. 1-3e, $p < 0.05$). The cellular fluorescence intensity with 25 μM methanol at 4 h was significantly higher than that without methanol ($p < 0.01$). The cellular fluorescence intensity without methanol at 6 h was distinguishable only from that at 2.5 × 10^3 μM methanol ($p < 0.05$).

Analysis of distribution and dose response of the cellular fluorescence intensity

Cellular adaptation to methanol is not necessarily homogenous in the population. I applied FACS analysis to examine the distribution of cellular fluorescence intensity in response to methanol dose to determine if individual cells with high fluorescence intensity are indeed sensing a high dose of methanol.

First, single yeast cells were separated from other particles and dividing cells or multiple cells through a gating strategy based on the forward and side scatter (Fig 1-4a-c, cf. Fig. 1-4 legends for details). At least 30,000 cells were analyzed per sample. I found that Venus fluorescence was proportional to the forward scatter, which reflects cell size (Fig. 1-4d). Thus, Venus fluorescence normalized to the forward scatter (Venus-A/FSC-A) was considered to represent the fluorescence intensity of a single cell.

Next, I analyzed the distribution of the Venus-A/FSC-A value of the sensor cells induced by various methanol concentrations. Virtually all cells showed a basal level of Venus-

A/FSC-A value without methanol (Fig. 1-4e, left). As the methanol concentration increased, I observed increasing numbers of cells with Venus-A/FSC-A values above the maximum level without methanol. Thus, the cellular response to methanol was not uniform in the population; nevertheless the number of cells with an increased Venus-A/FSC-A value was positively correlated with the methanol dose. In addition, the mode and the tail of the distribution shifted to higher Venus-A/FSC-A values as the methanol concentration increased up to 2.5×10^4 μM. For quantitative evaluation of the dose-response of the population, I used the geometric mean of Venus-A/FSC-A values, and found that this value increased up to 2.5×10^5 μM methanol (Fig. 1-4e, right).

To examine the cellular fluorescence intensity at low concentrations of methanol, I gained sensitivity of fluorescence detection by increasing the PMT voltage for Venus fluorescence. I found that the mode and the tail of the distribution of the Venus-A/FSC-A value shifted higher even at 2.5 μM methanol (Fig. 1-4f, left) , showing a detection limit of 2.5 μM (Fig. 1-4f (right), $p < 0.01$). Thus, FACS analysis of the optimized methanol sensor resulted in the detection of methanol at micromolar concentrations (Fig. 1-4 e and f).

Discussion

In this chapter, I developed a *K. phaffii* single-cell methanol sensor. The detection limit for methanol was improved by selection of the methanol-inducible promoter and the genetic background, and optimization of the assay conditions. Application of FACS enabled us to analyze fluorescence from ~30,000 single cells, > 100 times more than with fluorescence microscopy. To my knowledge, this is the first report of the distribution of methanol-induced protein production at a single-cell level. Through these analyses, I revealed the relationship between the distribution of cellular fluorescence and methanol dose, and found that the distributions of cellular fluorescence in the presence and absence of micromolar amounts methanol were clearly distinguishable. The detection limit of 2.5 μM is 100-fold lower than that of a similar fluorescent microscopy-based *C. boidinii* methanol sensor (Kawaguchi et al. 2011), and comparable to that of gas chromatography (Pontes et al. 2009).

The methanol-inducible promoter affected the detection limit of the methanol sensor cells. In the presence of glucose, methanol-inducible genes are completely repressed (Tschopp et al. 1987). In the absence of glucose or other repressing carbon sources, the expression level is elevated regardless of the presence of methanol. This methanol-independent gene activation is referred to as “de-repression”. On the other hand, methanol-dependent gene activation is called methanol induction, and results in a greater gene expression level than de-repression (Yurimoto et al. 2011). The desired characteristics of the promoter in the methanol sensor are a low level of de-repression and high level of methanol induction. The levels of de-repression and methanol induction differ among methanol-inducible promoters (Sakai et al. 1996; Vogl et al. 2016; Yurimoto et al. 2000). The level of de-repression with the alcohol oxidase (AOX)-encoding gene promoter was reported to be higher than that of the dihydroxyacetone synthase (DAS)-encoding gene promoter, while the level of methanol induction of the DAS-encoding

gene promoter was higher than that of the AOX-encoding gene promoter (Tschopp et al. 1987; Yurimoto et al. 2000). Also, the DAS-encoding gene is known to be fully activated at an earlier stage during methanol induction than the AOX-encoding gene in another methylotrophic yeast, *C. boidinii* (Sakai et al. 1996). My present results confirmed the superiority of the *DAS2* promoter over the *AOX1* promoter for use in the methanol sensor.

The physiological state of sensor cells was also found to be important for the detection of low concentrations of methanol. Release from glucose repression is a prerequisite for methanol induction (Yurimoto et al. 2000; Yurimoto et al. 2011). During preculturing on glucose medium, glucose completely represses methanol-inducible gene expression until mid-exponential phase. However, glucose repression is gradually attenuated as glucose is consumed during growth, so late-exponential phase cells are assumed to be more de-repressed than mid-exponential phase cells (Fig. 1-3a and 1-3b). Therefore, the physiological state of late-exponential phase cells is suitable for a sensitive response to low concentrations of methanol.

Taken together, the present methanol sensor was tuned up for detection of micromolar level of methanol from the aspects of the regulation of methanol metabolism in *K. phaffii*, which would be applicable for low concentration of methanol produced by methanol-producing enzymes. It is noteworthy that the established analysis of population-dynamics is applicable to elucidate the mechanism of methanol-inducible gene expression in *K. phaffii*.

Chapter II

Single-cell visualization of methanol-producing enzyme activity with yeast methanol sensor

Section I

Visualization of heterologous pectin methylesterase activity

Introduction

In Chapter I, I developed a *K. phaffii* single-cell methanol sensor that has a micromolar level of the lower detection limit. I considered that, when the methanol sensor cells are expressing a heterologous methanol-producing enzyme, each single cell gains fluorescence intensity that is proportional to the amount of methanol produced by the single cell. Therefore, I assumed that each single methanol sensor cell functions as an indicator of the methanol-producing enzyme activity of the cell itself. If this type of assay is established, a single cell having high activity, thus having high fluorescence intensity, can be readily distinguished and isolated by using FACS technology, from a population that has a heterogeneity in the activity. As $10^4 \sim 10^5$ cells can be sorted per minute on FACS, this could be a powerful strategy for the mass screening of transformants containing an enzyme gene library for high activity and/or stability.

In this section, I sought a methodology of the single-cell enzyme assay using the methanol sensor. As the model methanol-producing enzyme, I selected *Aspergillus niger* PME (Kawaguchi et al. 2011), an extracellular enzyme that hydrolyzes methyl-esterified pectin to polygalacturonate and methanol. The enzyme assay conditions for the methanol sensor would

be quite different from the conditions for detection of exogenous methanol present at the start of incubation, in that the concentration of methanol may change during cellular metabolism. I confirmed that the methanol sensor could detect methanol produced by PME activity, even though the concentration of methanol may not have reached the detection limit at any point. This result shows the feasibility of the methanol sensor for evaluating the activity of methanol-producing enzymes.

Materials and methods

Strains and media

The yeast strains used in this study are listed in Table 2-1-1. *K. phaffii* cells were grown at 28°C on glucose medium (1% yeast extract, 2% peptone, 2% glucose). The assay medium for detection of PME activity (PME assay medium) contained 0.67% yeast nitrogen base without amino acids and 0.05% pectin (esterified, from citrus fruit, Sigma, St. Louis, MO). All of the components in these media other than carbon sources were purchased from Becton Dickinson. Cell growth was monitored by the optical density at OD_{610}.

Plasmid construction and transformation

The oligonucleotide primers used in this study are listed in Table 2-1-2. The plasmids used in this study are listed in Table 2-1-3. To construct pGAPZPME, a 996-bp DNA fragment corresponding to the deduced amino acid sequence of the *A. niger pmeA* gene (Kawaguchi et al. 2014), which includes an N-terminal secretory signal peptide, was inserted into the EcoRI/NotI sites of pGAPZB in frame with a C-terminal His_6-tag encoding sequence in the

Table 2-1-1 Yeast strains used in this study

Strain	Genotype	Description	Source or reference
PMT1302	PMT1301 *arg4*::pNT204 (*ARG4*)	Non-auxotrophic methanol sensor strain	Chapter I
PMT1303	PMT1302 P_{GAP}::pGAPZPME (P_{GAP}-PME-His_6 *Sh ble*)	Methanol sensor strain with a single copy of PME-His_6	This study
PMT1304	PMT1303 P_{GAP}::pGAPBPME (P_{GAP}-PME-His_6 *Blasticidin*)	Methanol sensor strain with two copies of PME-His_6	This study

Table 2-1-2 Oligonucleotide primers used in this study

Primer	Sequence (5'-3')	Purpose
PME-FL-Nt-EcoRI	CGAGGAATTCAAACGATGGTT AAGTCAATTCTTGCATCT	Amplification of *A. niger pmeA* for construction of pGAPZPME
PME-Ct-NotI	GGCGGCCGCGTTGATGTAACT AGTATCAACCCAATC	
PGAP-SB-F	AAATGTCTTGGTGTCCTCGT	Amplification of 0.4-kb DNA fragment within the *GAP* promoter region in the *K. phaffii* genome for preparation of a DNA probe for Southern blot analysis
PGAP-SB-R	CAAAATTGGGAAAGGTGTTC	

plasmid. The PME-His_6 expression cassette of pGAPZPME was excised with NsiI and BamHI and inserted into the PstI/BamHI sites of pTEF1/Bsd to obtain pGAPBPME. pGAPZPME and pGAPBPME were linearized at the AvrII site for transformation. *K. phaffii* cells were transformed by electroporation as described previously (Wu and Letchworth 2004).

Table 2-1-3 Plasmids used in this study

Plasmid	Description	Source or reference
pGAPZB	$Zeocin^R$; P_{GAP}-based expression vector	Invitrogen
pGAPZPME	*A. niger pmeA* inserted into EcoRI/NotI sites of pGAPZB in frame with a C-terminal His_6-tag sequence	This study
pTEF1/Bsd	$Ampicillin^R$, $Blasticidin^R$	Invitrogen
pGAPBPME	P_{GAP}-PME-His_6 expression cassette of pGAPZPME inserted into PstI/BamHI sites of pTEF1/Bsd	This study

Southern blot analysis

To prepare a DNA probe for detecting the PME-His_6 expression cassettes, a 0.4-kb DNA fragment within the *GAP* promoter region from the *K. phaffii* genome was amplified by PCR using the primer set PGAP-SB-F / PGAP-SB-R. This DNA fragment was labeled with alkaline phosphatase using AlkPhos Direct Labelling Module (GE Healthcare Bio Science, Waukesha, WI). Yeast DNA was isolated as described previously (Davis et al. 1980). Isolated genomic DNA was digested with BamHI or AflII and electrophoresed on a 0.7% agarose gel. Fractionated DNA was blotted onto a Hybond-N+ (GE Healthcare) membrane saturated with 20× SSC (3M NaCl, 0.3M sodium citrate, pH 7.0) by the capillary transfer technique. The DNA on the membrane was fixed by baking at 80°C for 2 h. Hybridization with the labeled DNA probe was performed at 55°C. Bound probe was detected using CDP-*star* detection reagent (GE Healthcare) and the signal was analyzed with a Light Capture System (ATTO, Tokyo, Japan).

Flow cytometry

Flow cytometry was conducted as described in “Materials and methods” section of Chapter I except that Venus fluorescence was detected at a PMT voltage of 700.

Immunoblot analysis

Cells were grown in glucose medium and the amount of PME-His_6 secreted into the supernatant was analyzed as follows. The supernatant was mixed with 3× sample buffer (50 mM Tris-HCl pH 6.8, 30% glycerol, 3% SDS, 3% 2-mercaptoethanol, a dash of bromophenol blue) and boiled for 5 min. Resulting samples were electrophoresed on a 12% SDS-PAGE gel. Proteins were transferred onto a PVDF membrane by semidry blotting (Bio-Rad, Richmond, CA). The blot was blocked and incubated with anti-His-tag mAb-HRP-DirecT antibody (Medical & Biological Laboratories, Nagoya, Japan) at a 1:10,000 dilution for 1 h. Bound HRP-conjugated

antibody was detected using Western Lightning (Perkin-Elmer Life Science, Waltham, MA) and the signal was analyzed with a Light Capture System (ATTO). PME-His_6 signal intensity was quantified using CS Analyzer software (ATTO).

PME enzyme activity assay

PME enzyme activity in the culture broth was determined as described previously (Anthon and Barrett 2004) with slight modifications. The reaction mixture contained 10 mM citrate buffer (pH 4.0), 0.5% (w/v) pectin and an appropriate amount of culture broth. This mixture was kept at 28°C and 100 µL was sampled at several time points and placed on ice to stop the reaction. Samples were mixed with an equal volume of 20 unit/mL alcohol oxidase (from *P. pastoris*; Sigma) in 100 mM HEPES-KOH pH 8.0 and incubated at 37 °C for 10 min to oxidize the produced methanol to formaldehyde. The resulting mixture was mixed with an equivalent volume of 5 mg/mL Purpald (4-amino-3-hydrazino-5-mercapto-1,2,4-triazole) dissolved in 0.5 N NaOH. The condensation of formaldehyde and Purpald results in the formation of a cyclic aminal, which is subsequently oxidized to form a purple tetrazine dye. After 30 min of incubation at room temperature, absorbance at 550 nm was determined. A standard curve was generated from known concentrations of methanol. One unit of activity was defined as the amount of enzyme that produced 1 µmol of methanol per min.

Results

Application of the methanol sensor for the detection of methanol-producing heterologous PME activity

The enzyme assay conditions were established as follows. First, the methanol sensor cells harboring the gene encoding a methanol-producing enzyme under the control of the constitutive *GAP* promoter (P_{GAP}) were precultured in glucose medium. At this stage, the enzyme is highly expressed under P_{GAP}, but expression of the Venus-PTS1 gene under P_{DAS2} is repressed. The cells were then transferred into enzyme assay medium containing the substrate. Methanol produced from the substrate and its metabolism induce Venus-PTS1 during 4 h of incubation (Fig. 2-1-1).

I constructed expression vectors for the *A. niger* PME tagged with 6×His at the C-terminus under the control of P_{GAP}, and introduced them into the methanol sensor strain constructed in Chapter I. I obtained single- and two-copy strains as revealed by Southern blot

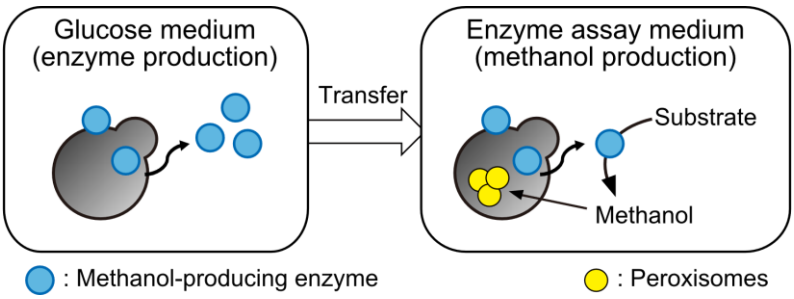

Fig. 2-1-1 Schematic illustration of methanol sensor-based evaluation of PME activity. Cells from glucose medium were washed and transferred to PME assay medium. Since PME-His_6 is expressed from a constitutive promoter, PME-His_6 synthesized before and/or after medium shift is secreted into the PME assay medium. Secreted PME-His_6 hydrolyzes the methylester group of pectin, producing methanol, which is expected to increase the cellular fluorescence intensity.

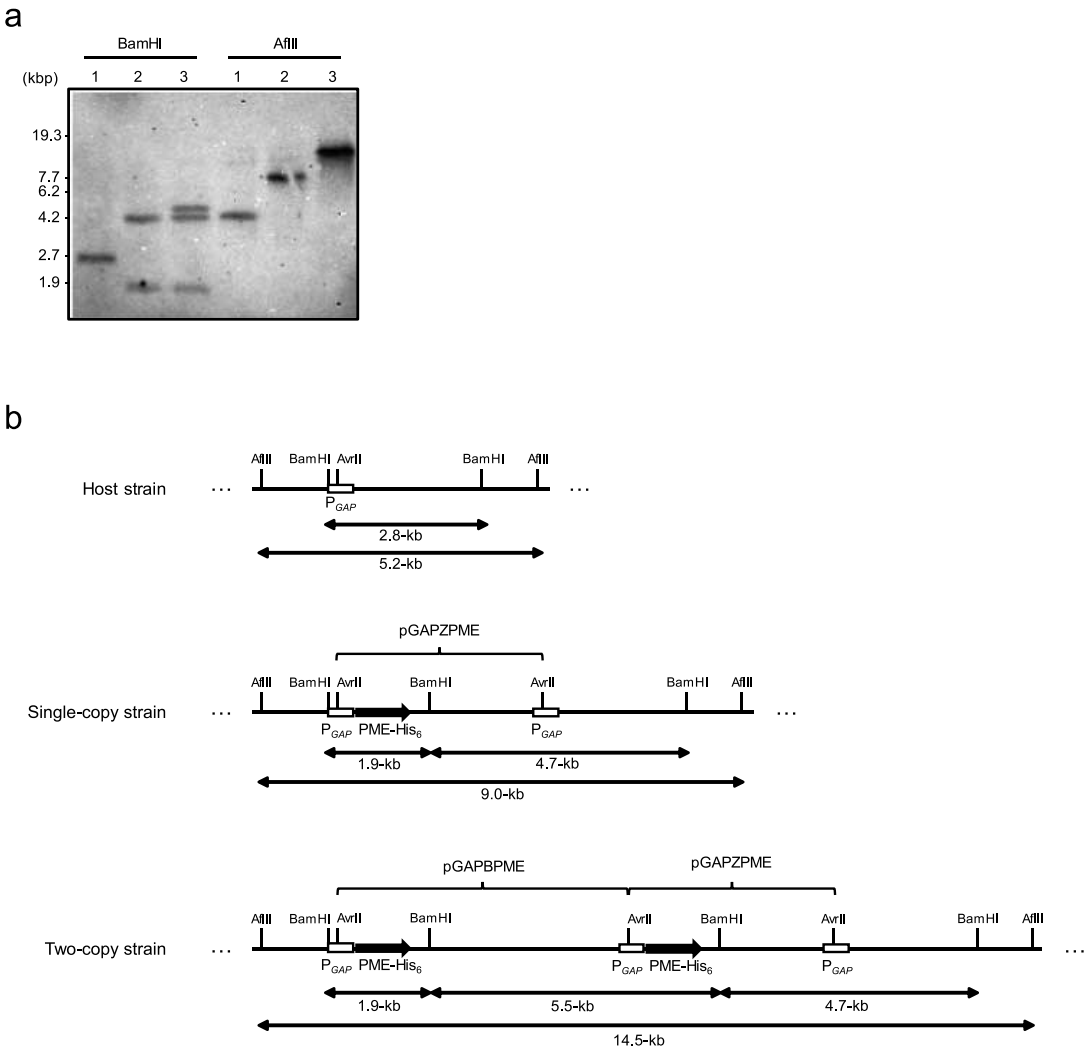

Fig. 2-1-2 Southern blot analysis of the PME-His_6 expression cassette. **a** Genomic DNA from the host sensor strain PMT1302 (lanes 1), strain PMT1303 (PMT1302 transformed with pGAPZPME) (lanes 2), and strain PMT1304 (PMT1303 transformed with pGAPBPME) (lanes 3), were digested with the indicated restriction endonucleases. The DNA fragments containing the PME expression cassette were detected using the DNA probe (the *GAP* promoter region). **b** The diagram shows the structure of the *GAP* locus of the host sensor strain (accession no. FN392320) and those of the single- and two-copy strains. For the host strain, BamHI and AflII digestion resulted in single 2.8- and 5.2-kb bands, respectively, which are consistent with the genome sequence data. With the single-copy strain, BamHI-digestion resulted in two 1.9- and 4.7-kb bands, and AflII-digestion resulted in a 9.0-kb band, confirming that a single copy of pGAPZPME was inserted at the *GAP* locus. With the two-copy strain, BamHI-digestion resulted in a 5.5-kb band in addition to the bands of the single-copy strain, and AflII-digestion resulted in a 14.5-kb band, confirming that a single copy of pGAPBPME was additionally inserted at the *GAP* locus of the single copy strain PMT1303.

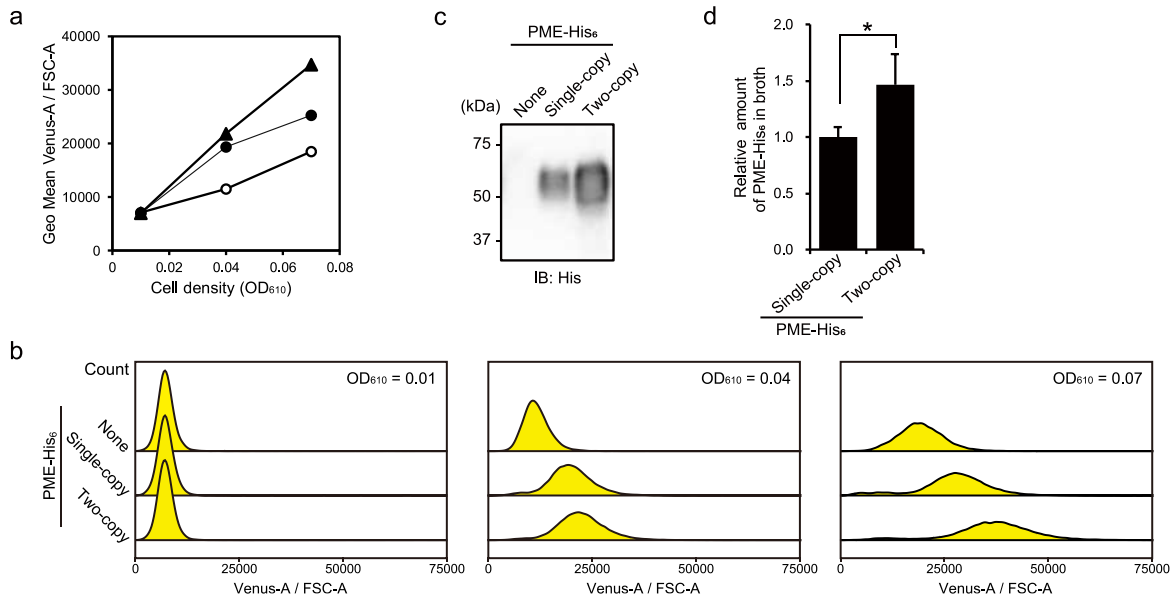

Fig. 2-1-3 Production of His_6-tagged *A. niger* PME in the methanol sensor host. **a** FACS analysis of the host methanol sensor cells (open circles), the cells harboring one- and two-copies of PME-His_6 (closed circles and closed triangles, respectively) incubated in PME assay medium. Cells were precultured in glucose medium to late-exponential phase (see Chapter I), transferred to PME assay medium, and incubated for 4 h. At least 30,000 cells were measured at a Venus PMT voltage of 700. **b** Distribution of the Venus-A/FSC-A values of cells in **a**. **c** Secretion of PME-His_6 detected by immunoblotting. Cells were grown in glucose medium for 30 h, and samples prepared from equal volumes of supernatant were loaded in each lane. **d** Densitometry of three biological replicates of immunoblot analyses as **c**. For **d**, error bars represent means ± standard deviations of samples from three independent cultures. Statistical significance was calculated by two-tailed Student's *t* test assuming equal variance (n.s., $p > 0.05$; *, $p < 0.05$).

analysis (Fig. 2-1-2). Next, these strains were grown on glucose medium to late-exponential phase, transferred to PME assay medium, and incubated for 4 h. During this period, PME-His_6 synthesized before and/or after transfer is secreted into the PME assay medium. The cell density in the PME assay medium was set below an OD_{610} of 0.1 to prevent exhaustion of the substrate, i.e., methylester groups of pectin. According to FACS analysis, cells expressing PME-His_6

Table 2-1-4 PME enzyme activities in culture broth of the methanol sensor and transformant strains

PME expression	None	Single copy	Two-copy
Activity[a] (units/mL broth)	n.d.[b]	16.2 ± 4.6	29.7 ± 0.4

[a]Means ± standard deviations of three measurements.

[b]Not detected (< 7.41×10^{-2} units/mL broth).

showed a cell density-dependent increase in the geometric mean of the Venus-A/FSC-A value (Fig. 2-1-3a). I noted that the host sensor cells also showed a relatively moderate increase in the geometric mean of the Venus-A/FSC-A value, which was ascribed to the endogenous PME activity (Kawaguchi et al. 2014; Nakagawa et al. 2005). The two-copy strain showed a higher geometric mean of the Venus-A/FSC-A value than cells containing a single-copy. In addition, the mode and the tail of the distribution of the Venus-A/FSC-A value increased with increasing amounts of enzyme, i.e., the cell density or the copy number (Fig. 2-1-3b). In contrast, the methanol sensor did not give significant increase of fluorescence with polygalacturonate (another product of PME-catalysis). Therefore, the Venus-A/FSC-A value was assumed to represent pectin-dependent methanol formation.

I next biochemically confirmed the production of PME-His_6 in these strains by immunoblot analysis. In both PME-containing strains, I detected broad bands of 50 to 60 kDa that were attributed to PME-His_6 (Fig. 2-1-3c). Although this band size disagrees with the estimated value from the amino acid sequence of the processed form of PME-His_6, glycosylation via the secretion pathway was assumed to result in the increased molecular weight. The band of PME-His_6 from the two-copy strain was more intense than that from the single-copy strain; the two-copy strain produced ca. 1.5 times PME-His_6 (Fig. 2-1-3d). In addition,

PME enzyme activity in the broth of the two-copy strain was about 1.8 times greater than that of the single-copy strain (Table 2-1-4), which is consistent with the production level of PME-His_6. Hence, the PME-His_6 gene copy number reflected the PME-His_6 production and activity level. From these results, I concluded that methanol sensing by single cells was successful for evaluating the activity of a heterologously expressed methanol-producing enzyme, and could discriminate the 1.5-fold difference in PME activity between the two strains.

Discussion

In this chapter, the *K. phaffii* methanol sensor was used as the expression host for the heterologous methanol-producing enzyme, PME. The detection limit of the methanol sensor was confirmed to be sufficient for evaluation of the produced enzyme activity. It is unlikely that the methanol concentration rose above the detection limit soon after the start of incubation of sensor cells with the substrate. I assume that the methanol sensor cells not only responded to the methanol concentration at the start of the enzyme reaction, but also monitored further methanol metabolism for induction and synthesis of the Venus-PTS1 protein, because *aox1*Δ cells impaired in methanol metabolism showed lower cellular fluorescence intensity than the wild-type cells (see Chapter I). Indeed, not only methanol but also the downstream metabolites formaldehyde and formate induced fluorescence from the methanol sensor cells (Sakai et al. 1999) (data not shown). These properties are ideal for the detection of very weak methanol-producing enzyme activity with the host *K. phaffii* cells.

Since the level of cellular enzyme activity correlated with the maximum level of cellular fluorescence, highly active cells could be selected and isolated by FACS. Such screening cannot be achieved by a methanol sensor constructed with microbial cells immobilized on an oxygen electrode (Wen et al. 2014). This study demonstrates the feasibility of a high-throughput screen for cells with high methanol-producing enzyme activity with the methanol-sensing system developed in Chapter I, which will play a key role in engineering of an enzyme mutant with high specific activity and/or stability.

Section II

Visualization of methane oxidation reaction in cell reaction

Introduction

As mentioned earlier, methanol is currently and mainly produced from methane, a main component of natural gas, via syngas. Although direct production of methanol from methane has been a long-time focus in industry, development of catalysts that can activate extremely inert C-H bond of methane (ΔH_{298} = 105 kcal/mol) and can selectively oxidize it to methanol is still challenging in the fields of chemistry.

On the other hand, in nature, methane-to-methanol oxidation is carried out with high selectivity and reaction rate by a variety of MOBs including MMOs, or microbial cells expressing MOBs (MOB cells). There exist two distinct types of MMO: a soluble cytoplasmic MMO (sMMO), and a membrane-bound particulate MMO (pMMO). Both oxidize methane at metal centers within a complex, multisubunit scaffold, but their structures and metal cofactors are completely different (Chan and Lee 2019; Ross and Rosenzweig 2017; Sirajuddin and Rosenzweig 2015). Much attention has been paid to MOBs because understanding their catalytic mechanisms would aid development of novel methane-oxidizing catalysts and biotechnological use of them would promote utilization of methane in bioindustry. However, these approaches have been hindered because functional expression of MOBs in heterologous hosts has not been successful (Clomburg et al. 2017).

In this section, I describe visualization of biological methane oxidation activity with the *K. phaffii* methanol sensor, which would facilitate the development of MOBs that can be functionally expressed in heterologous hosts by methane oxidation activity-based screening of

engineered or naturally occurring MOB genes. I used a gram-positive bacterium *Mycolicibacterium* sp. TY-6 (recently reclassified from *Mycobacterium* sp. TY-6) as model MOB cells. This bacterial strain was previously isolated in my laboratory as a propane utilizer (Kotani et al. 2006). This bacterium can utilize C3-C9 and C10-C19 *n*-alkanes, but not methane, as the sole carbon source, nevertheless, showed methane oxidation activity and accumulated methanol in cell reaction (unpublished data). The *K. phaffii* methanol sensor co-cultured with *Mycolicibacterium* sp. TY-6 showed increase of fluorescence intensity in the presence of methane, successfully establishing the methanol sensor as a means for detection of methane oxidation activity. I subsequently used the methanol sensor as an expression host for natural and artificial MOB genes, however, could not consistently detect the methane oxidation activity. This inconsistency led me to investigate non-enzymatic oxidation of methane, and I found that the reaction can be caused by duroquinol (tetramethylhydroquinone), which was used as a reductant for pMMO-derived artificial MOB assay, or H_2O_2, which can be produced by duroquinol, in phosphate buffered saline (PBS) buffer. These results will guide engineering, exploitation and mechanistic understanding of MOBs or MOB cells, with awareness of non-enzymatic artifacts.

Materials and methods

Microbial strains and media

The yeast strains used in this study are listed in Table 2-2-1. *K. phaffii* cells were grown at 28°C on glucose medium (1% yeast extract, 2% peptone, 2% glucose). *Mycolicibacterium* sp. TY-6 cells (Kotani et al. 2006) were grown at 28°C on Luria-Bertani (LB) medium. 0.67% yeast nitrogen base without amino acids (YNB medium) (Becton Dickinson) was used for the medium for co-culture of *K. phaffii* and *Mycolicibacterium* sp. TY-6. Cell growth was monitored by the optical density at OD_{610}.

Plasmid construction

The oligonucleotide primers used in this study are listed in Table 2-2-2. The plasmids used in this study are listed in Table 2-2-3. pACTBmC was constructed by assembling 0.9-kb upstream region of the *ACT1* gene, mCherry gene and 0.3-kb transcription terminator region of the *AOX1* gene by overlap-extension PCR, and ligating the assembled fragment into BamHI/EcoRI sites of pTEF1/Bsd. pACTBmC was linearized at the AvrII site for transformation. *K. phaffii* cells were transformed by electroporation as described previously (Wu and Letchworth 2004).

Table 2-2-1 Yeast strains used in this study

Strain	Genotype	Description	Source or reference
PMT1302	PMT1301 *arg4*::pNT204 (*ARG4*)	Non-auxotrophic methanol sensor strain	Chapter I
PMT1305	PMT1301 P_{ACT1}::pACTBmC (P_{ACT1}-mCherry *Blasticidin*)	Methanol sensor strain labeled with mCherry	This study

Table 2-2-2 Oligonucleotide primers used in this study

Primer	Sequence (5'-3')	Purpose
P(PpACT1)-F-EcoRI	AGCTGAATTCTATGTCGCTGGTAATCCCGG	Amplification of 0.9-kb upstream region of the *ACT1* gene for construction of pACTBmC
P(PpACT1)-R-mCherry-Nt	CCTTGCTCACCATTTTTGTATTGATGAATTTCTTTTACTAAACTGTTTC	
mCherry-F-P(PpACT1)-3-	TCATCAATACAAAAATGGTGAGCAAGGGCG	Amplification of mCherry gene for construction of pACTBmC
mCherry-R-PpAOX1TT-5-	GTCTAAGAAGCTTCTACTTGTACAGCTCGTCCAT	
PpAOX1TT-F-mCherry-Ct	GCTGTACAAGTAGAAGCTTCTTAGACATGACTGTTCC	Amplification of 0.3-kb transcription terminator region of the *AOX1* gene for construction of pACTBmC
PpAOX1TT-R-BamHI	AGAGGATCCTGTGGGAAATACCAAGAAAAACATC	

Co-culture of *K. phaffii* and *Mycolicibacterium* sp. TY-6

K. phaffii cells were grown to late-exponential phase (see Chapter I) on glucose medium. *K. phaffii* cells and *Mycolicibacterium* sp. TY-6 cells were washed twice with and resuspend in ice-cold YNB medium. The final OD_{610} of *K. phaffii* was set at 0.01 and that of *Mycolicibacterium* sp. TY-6 was changed. *Mycolicibacterium* sp. TY-6 cell suspensions without

Table 2-2-3 Plasmids used in this study

Plasmid	Description	Source or reference
pTEF1/Bsd	$Ampicillin^R$, $Blasticidin^R$	Invitrogen
pACTBmC	P_{ACT1}-mCherry expression cassette inserted into BamHI/EcoRI sites of pTEF1/Bsd	This study

K. phaffii cells were used for determination of methane oxidation activity (see below). Five mL of the cell suspension was transferred into a 25-mL sealed glass vial, into which 5 mL of methane or nitrogen gas (GL Sciences, Tokyo, Japan) was injected. The vials were incubated at 28°C for 6 h and subsequently placed on ice to stop the cell reaction.

Flow cytometry

Flow cytometry was conducted as described in "Materials and methods" section of Chapter I except the following. FSC was detected at a PMT voltage of 150 with a threshold of 500. Venus fluorescence was detected at a PMT voltage of 730. mCherry fluorescence was excited with a 500 nm laser and the emission at 610/20 nm was detected at a PMT voltage of 500. Cells were gated for FSC, SSC and mCherry fluorescence to select single *K. phaffii* cells as shown in Fig. 2-2-1. Venus fluorescence intensity (Venus-A) and mCherry fluorescence intensity (mCherry-A) normalized to FSC-A (Venus-A/FSC-A and mCherry-A/FSC-A) with 10% and 75% scaling, respectively, were used to represent the fluorescence intensity of each cell. At least 10,000 *K. phaffii* cells were analyzed per sample. FlowJo software (Becton Dickinson) was used for processing FCS data for preparation of histograms.

Examination of production of methanol from methane by *Mycolicibacterium* sp. TY-6 cells

Density of the cell suspensions (see above) was OD_{610} of 2.5. One mL of the cell suspension was sealed in a 7.7-mL glass vial. Ca. 1.68 mL of methane or nitrogen gas was injected into the vial. The vials were incubated at 28°C for 6 h and subsequently placed on ice to stop the cell reaction.

The methanol concentration in the supernatant was determined using a GC-2014 (Shimadzu, Kyoto, Japan) gas chromatograph equipped with a flame ionization detector and InertCap Pure-WAX column (60 m × 0.53 mm i.d. × 1.0 μm, GL Sciences). Three μL of the

sample was injected. Nitrogen gas was used as the carrier. The temperature program of the oven was 40°C for 5 min, then a ramp of 20°C min^{-1} to 240°C (held for 15 min), and the injector and detector were set at 240°C.

Non-enzymatic oxidation of methane

Ultrapure water with the resistivity of 18.2 MΩ・cm at 25°C was used throughout the experiments. The reaction mixture (250 μL) consisted of 5 mg of duroquinol or 500 mM H_2O_2 in PBS buffer. Duroquinol was prepared and stored as described previously (Zahn and DiSpirito 1996). Composition of PBS buffer was the same as that used for the previous methane oxidation assay (137 mM NaCl, 2.7 mM KCl, 10 mM Na_2HPO_4, 1.8 mM KH_2PO_4, pH 7.4) (Ross et al. 2019). The reaction mixture was prepared in a 7.7-mL sealed glass vial. Subsequently, 2.5 mL of air and 5.0 mL of ^{13}C-methane (Shoko Science, Yokohama, Japan) or nitrogen gas were injected into the vial. The vial was immediately placed at 28 or 35 °C to start the reaction, and shaken at 120 spm. To stop the reaction, the reaction mixture was centrifuged at 20,000 × *g* for 2 min at 4°C, and the resulting supernatant was frozen in liquid nitrogen. This step took approximately 10 min. Samples were stored at -80°C until GC/MS analyses.

The ^{13}C-methanol concentration in the sample was determined using gas chromatography-mass spectrometry (GC/MS system, GCMS-QP2010 Ultra, Shimadzu) with Nukol^{TM} column (30 m × 0.25 mm i.d. × 0.25 μm, Supelco, Bellefonte, PA, USA). Helium at a flow rate of 6.1 mL min^{-1} was used as carrier gas. One μL of the sample was injected. The injector temperature was set at 200°C. The temperature program of the oven was 40°C for 2 min, then a ramp of 20°C min^{-1} to 110°C (held for 5 min). MS was used with a source temperature of 200°C. 33 *m/z* ion was monitored for detection of ^{13}C-methanol.

Results

Synthesis of fluorescent protein with methane by a co-culture of the methanol sensor cells and *Mycolicibacterium* sp. TY-6 cells

Mycolicibacterium sp. TY-6 cells grown in LB medium could oxidize methane to methanol in cell reaction, and produced methanol accumulates in the reaction mixture (unpublished data). I cultured *Mycolicibacterium* sp. TY-6 cells in LB medium, resuspended the cells together with the *K. phaffii* methanol sensor cells in YNB medium in a sealed vial, into which methane was injected, to perform the co-culture of the two species and methane oxidation by *Mycolicibacterium* sp. TY-6 cells for 6 h. Subsequently, I subjected this co-culture to FACS analysis. I distinguished the methanol sensor cells, which had been labelled by expressing mCherry, from *Mycolicibacterium* sp. TY-6 cells, with a gating strategy based on FSC, SSC and mCherry fluorescence (Fig. 2-2-1). I found that the mode and the tail of the distribution of the Venus-A/FSC-A value increased with increasing density of *Mycolicibacterium* sp. TY-6 cells (Fig. 2-2-2a). Increase of the geometric mean of the Venus-A/FSC-A value correlated with the density of *Mycolicibacterium* sp. TY-6 cells in the presence of methane, which was not observed when nitrogen gas was injected instead of methane (Fig. 2-2-2b). The ability of *Mycolicibacterium* sp. TY-6 cells to oxidize methane to methanol was confirmed in the cell reaction which does not contain the methanol sensor cells, and the amount of methanol produced in the reaction was 42 ± 4 μM (mean ± standard deviation of triplicate reactions) with the density of OD_{610} of 2.5 of *Mycolicibacterium* sp. TY-6 cells. Methanol was not detected (peak not observed, < 25 μM) with nitrogen gas instead of methane. The fluorescence intensity of methanol sensor cells incubated with 50 μM methanol for 6 h was close to those co-cultured with the same density of *Mycolicibacterium* sp. TY-6 cells in the presence of methane (Fig. 2-2-2b and c). These results show that the methanol sensor cells produced Venus-PTS1 depending

on the amount of methanol produced from methane by *Mycolicibacterium* sp. TY-6 cells. Therefore, I succeeded in visualization of the methane oxidation activity of *Mycolicibacterium* sp. TY-6 cells. In addition, these results mean that this co-culture system can be used for one-pot production of protein (in this case Venus-PTS1) from methane.

Expression of MMO genes in the methanol sensor

As the methanol sensor could be used for detection of the methane oxidation activity in cell reaction, I next attempted to use the sensor cells as an expression host for MMO genes. Using *Methylovulum miyakonense* HT12 as a source of genes (Iguchi et al. 2010; Iguchi et al. 2011), I constructed expression vectors for MOB genes including sMMO genes and artificial MOB genes designed using sMMO and pMMO genes, and introduced them into the methanol sensor cells. In spite of intensive trials, I could not confirm methane oxidation activity of the MOB gene-expressing methanol sensor strains (data not shown). Particularly, in case of the artificial MOB genes derived from pMMO, the results were not consistent.

Analysis of non-enzymatic oxidation of methane by duroquinol or hydrogen peroxide

I considered that the inconsistency in the methanol sensor-based activity assay of the pMMO-derived artificial MOBs can be ascribed to non-enzymatic oxidation of methane for a following reason. As isolated pMMO was reported to require reduced quinone including duroquinol to supply reducing power (Shiemke et al. 1995), the *in vitro* assays in previous reports (Balasubramanian et al. 2010; Kim et al. 2019; Ross et al. 2019) and the methanol sensor-based assays in this study of artificial pMMO-derived MOBs also contained duroquinol. However, Ross et al. reported that duroquinol caused non-enzymatic oxidation of methane (Ross et al. 2019). This report proposed a following scheme: (1) Duroquinol reduces O_2 to H_2O_2. (2) H_2O_2 produces $OH^{\bullet}$ through autolysis and through Fenton and Haber-Weiss chemistry. (3) $OH^{\bullet}$

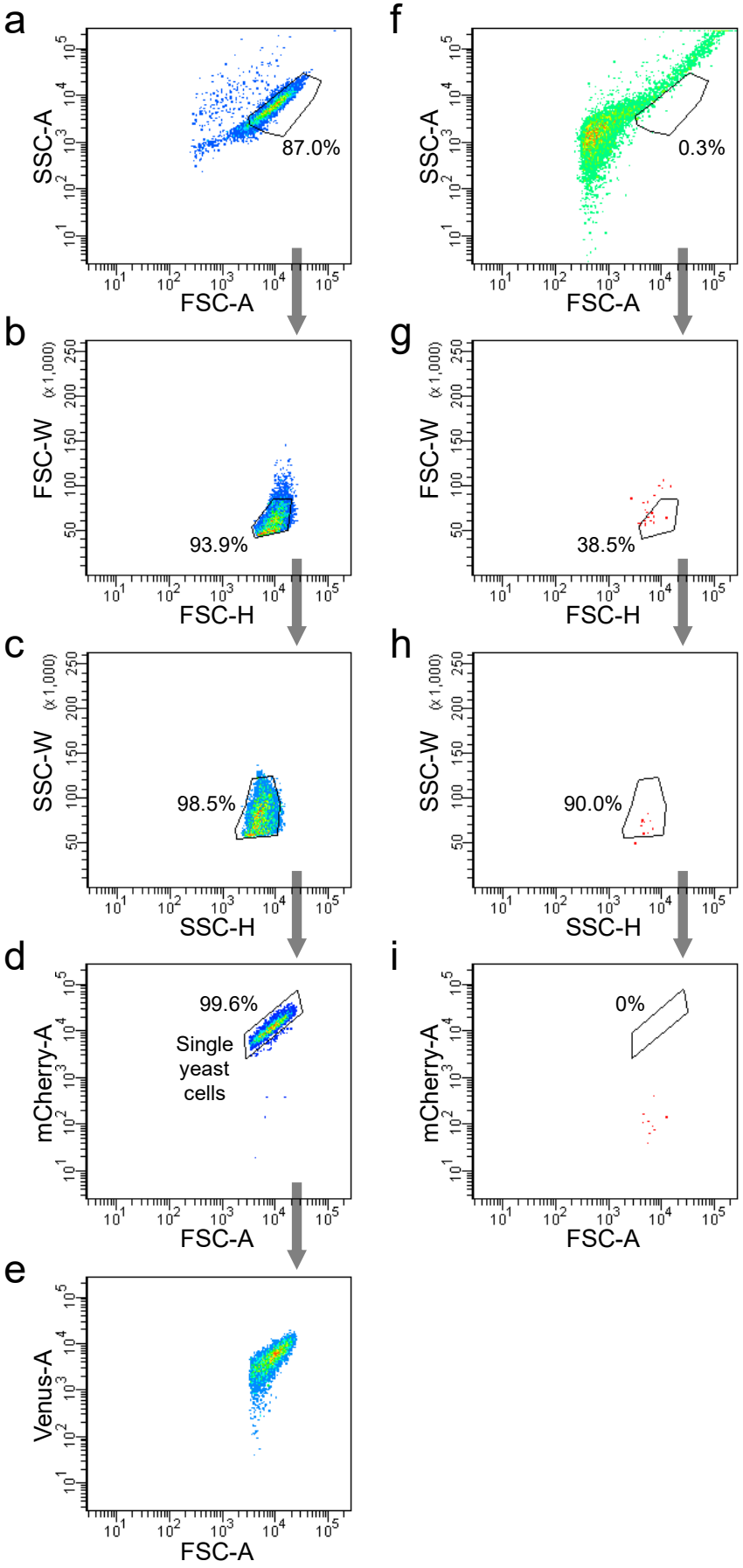
a
SSC-A
FSC-A
87.0%
b
FSC-W (x 1,000)
FSC-H
93.9%
c
SSC-W (x 1,000)
SSC-H
98.5%
d
mCherry-A
FSC-A
99.6%
Single yeast cells
e
Venus-A
FSC-A
f
SSC-A
FSC-A
0.3%
g
FSC-W (x 1,000)
FSC-H
38.5%
h
SSC-W (x 1,000)
SSC-H
90.0%
i
mCherry-A
FSC-A
0%

Fig. 2-2-1 A gating strategy for distinguishing single *K. phaffii* methanol sensor cells from *Mycolicibacterium* sp. TY-6 cells that was developed in advance to analyses of mixtures of the methanol sensor cells and *Mycolicibacterium* sp. TY-6 cells. Methanol sensor cells that were labelled by constitutive expression of mCherry and *Mycolicibacterium* sp. TY-6 cells were separately subjected to FACS analyses. According to the data, I developed the gating strategy in which the methanol sensor cells and the *Mycolicibacterium* sp. TY-6 cells appear as shown in **a**-**e** and **f**-**i**, respectively. The gates were based on FSC-A and SSC-A (**a** and **f**), FSC-H and FSC-W (**b** and **g**), SSC-H and SSC-W (**c** and **h**), and FSC-A and mCherry fluorescence area (mCherry-A) (**d** and **i**). Gates were used in this order. After the gating, no *Mycolicibacterium* sp. TY-6 cell was present within the gate shown in **i**. **e** shows a plot against FSC-A and Venus-A of the single methanol sensor cells selected with the gates **a**-**d**.

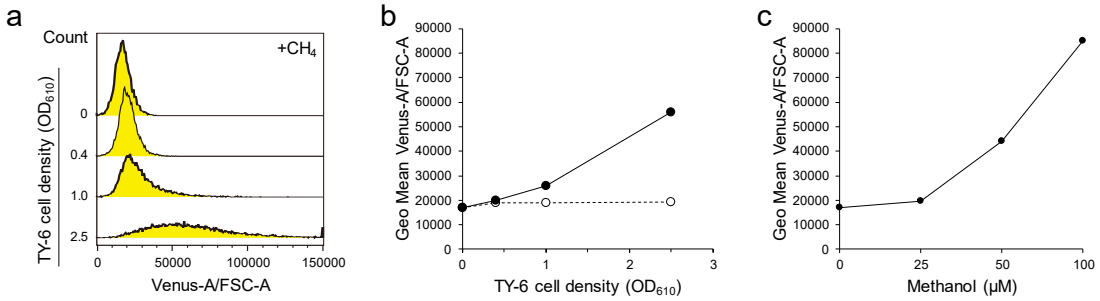

Fig. 2-2-2 FACS analyses of the synthesis of the fluorescent protein Venus-PTS1 with methane by the methanol sensor cells co-cultured with *Mycolicibacterium* sp. TY-6 cells that have methane oxidation activity. **a** Histograms of the Venus-A/FSC-A value of the co-cultured methanol sensor cells in the presence of methane. **b** Geometric means of the co-cultured methanol sensor cells in the presence of nitrogen gas (open circles) or methane (closed circles, data are the same as those shown in **a**). **c** Geometric means of the methanol sensor cells incubated with various concentrations of methanol for 6 h in the absence of *Mycolicibacterium* sp. TY-6 cells.

oxidizes methane. This report argued that this non-enzymatic production of methanol from methane was observed at 35-45°C, however, there can be a doubt on this observation as activation of methane was considered to be difficult at such low temperature.

To confirm if methane can indeed be oxidized in the condition described above, I conducted the same experiment as Ross et al. did. I suspended duroquinol in PBS buffer in a sealed vial, into which ^{13}C-methane was injected, and incubated the vial at 35°C for 4 h. I analyzed the amount of ^{13}C-methanol in the supernatant by GC/MS analysis, and detected a peak at the retention time of ^{13}C-methanol (2.6-2.7 min), which was not observed in the absence of ^{13}C-methane or duroquinol (Fig. 2-2-3a). This result shows that the non-enzymatic oxidation of methane is indeed caused by duroquinol at 35°C. The production of methanol was also observed at 28°C, indicating the possibility for the activation of methane at such low temperature (Fig. 2-2-3b). Next, I replaced duroquinol in the reaction with 500 mM H_2O_2. As a result, I observed production of ^{13}C-methanol at a level comparable to the case of duroquinol

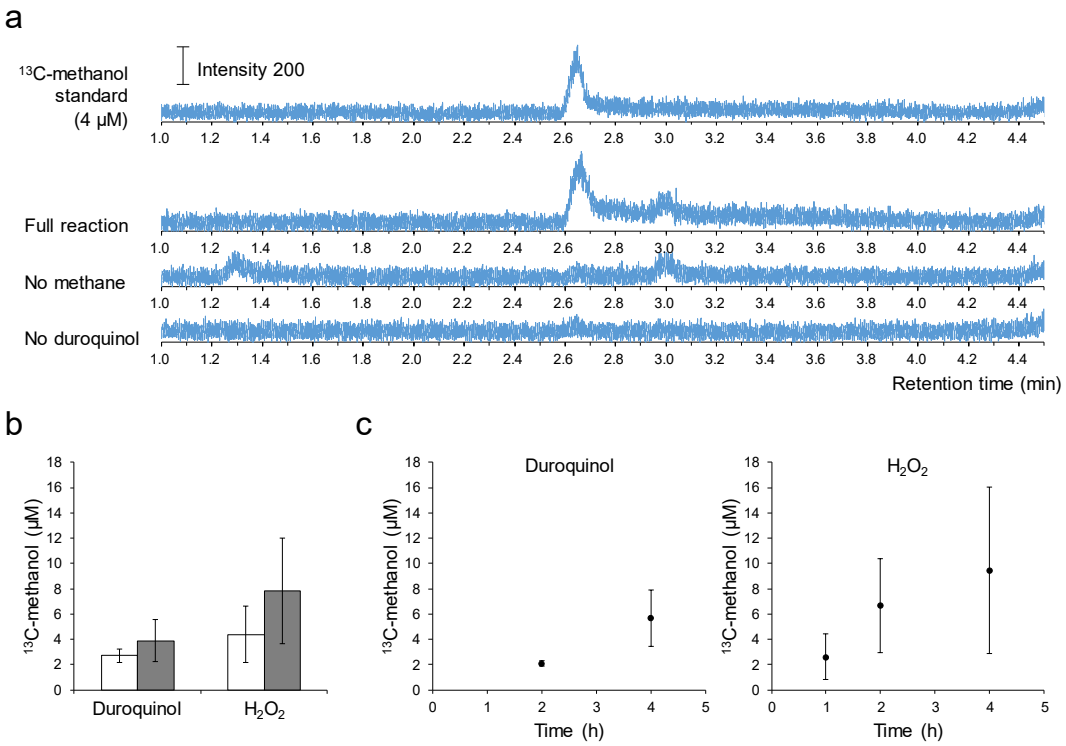

Fig. 2-2-3 Non-enzymatic oxidation of methane by duroquinol and H_2O_2. **a** GC/MS chromatograms of the non-enzymatic oxidation of methane by duroquinol at 35°C. The reactions were performed for 4 h. Full reaction, methane and duroquinol-containing reaction; No methane, ^{13}C-methane was replaced by nitrogen gas; No duroquinol, duroquinol-omitted reaction. **b** The amount of ^{13}C-methanol produced after 4 h of reactions with duroquinol or H_2O_2 at 28°C (open bars) or 35°C (gray bars). **c** Time-course analyses of the reactions at 35°C with duroquinol or H_2O_2. ^{13}C-methanol was not detected (< 1 μM) at t = 0 and 1 h for duroquinol-containing reaction and at t = 0 h for H_2O_2-containing reaction. In **b** and **c**, means ± standard deviations of triplicate reactions are shown.

(Fig. 2-2-3b). This result suggests the plausibility of the reaction scheme that involves reduction of O_2 to H_2O_2 by duroquinol. Finally, I conducted time-course analyses of the methanol production at 35°C, and found that the concentration of ^{13}C-methanol increased linearly for 4 and 2 h with duroquinol and 500 mM H_2O_2, respectively (Fig. 2-2-3c). The reaction rates estimated from the ^{13}C-methanol concentration at 2-4 h (duroquinol) and 1-2 h (H_2O_2) were 3.0 × 10^{-2} and 6.8 × 10^{-2} μM min^{-1}, respectively. These rates are comparable to the production of

methanol in the experiments of Ross et al. (around 10 μM for 1 h at 35°C) (Ross et al. 2019). These results show the importance of taking non-enzymatic reactions into account in interpreting results of activity assays for enzymatic oxidation of methane, particularly when H_2O_2 or other H_2O_2-producing reagents such as duroquinol is contained in the reaction.

Discussion

In this chapter, I showed that the methane oxidation activity of *Mycolicibacterium* sp. TY-6 cells could be visualized with the *K. phaffii* methanol sensor cells. The visualization of the methane oxidation activity at a single-cell level can facilitate the selection of a *K. phaffii* cell having high activity in combination with FACS technology. In addition, this result means that a heterologous protein (Venus-PTS1) was produced with methane in the co-culture of *Mycolicibacterium* sp. TY-6 and *K. phaffii*. To date, production of heterologous proteins from methane mainly relied on 3-pot synthesis that consists of methane-to-syngas and syngas-to methanol conversion followed by production of a target protein from methanol by methylotrophs. In contrast, the co-culture of *Mycolicibacterium* sp. TY-6 and *K. phaffii* achieves one-pot synthesis, providing an alternative means for production of heterologous proteins from methane. One-pot synthesis can also be achieved with methanotrophs, nevertheless, *Mycolicibacterium* sp. TY-6 has properties absent in methanotrophs, such as accumulation of methanol produced from methanol and an ability to utilize carbon sources except for methane. These properties are suitable for co-culture with another methanol-utilizing organism. Further understanding of methane oxidation machinery and development of genetic engineering methodologies in *Mycolicibacterium* sp. TY-6 will improve a feasibility of this co-culture system for production of various heterologous proteins and other value-added products.

The single-cell visualization of methane oxidation activity made it possible to explore MOBs that can be expressed in an active form in heterologous hosts. However, in this study, I could not identify or construct such MOB genes after screening of MOB genes in nature, design of artificial MOB genes for higher stability and activity, and intensive consideration of the concentration of metal ions that form the catalytic sites of MMOs. My investigations that are not presented here suggested that the majority of MOB gene products were produced as inactive

aggregates in the *K. phaffii* methanol sensor cells (data not shown), as previously reported for *E. coli* hosts (Balasubramanian et al. 2010; Clomburg et al. 2017). Therefore, I am convinced that not only the high-throughput screening system for active MOBs, but also concrete and in-depth investigations into the folding of MOBs in both methanotrophs and heterologous hosts, are necessary for heterologous expression of MOBs in an active form, a long-standing issue in MOB studies.

During the course of analyses on pMMO-derived artificial MOBs, I confirmed that duroquinol and H_2O_2 cause non-enzymatic oxidation of methane at room temperature. Although the reaction rates were low and side reactions were not investigated, these results show that methane can be oxidized to methanol under this mild condition and in the absence of a biological or artificial catalyst. This was an unexpected observation since the activation of extremely inert C-H bond of methane was unlikely to occur in such a condition, providing a new insight into the reactivity of methane. This finding will also shed a new light on the controversy in the previous studies on pMMO, where the catalytic center was argued to reside in the soluble domain of pmoB subunit after activity assays containing duroquinol (Balasubramanian et al. 2010; Kim et al. 2019). The reaction scheme is considered to involve $OH^{\bullet}$ produced from H_2O_2 (see "Results" section for the overall scheme), however, I did not add heavy metal ions, which are considered to be necessary for $OH^{\bullet}$ production from H_2O_2 via Fenton and Haber-Weiss chemistry, in the reactions. As the other $OH^{\bullet}$ production route, H_2O_2 autolysis, is less plausible in this condition, I assume that Fenton and Haber-Weiss chemistry was caused by a trace amount of heavy metal ions contained in the buffer or other reagents that is enough to drive the chemistry.

Taken together, this study is a significant step towards further engineering, exploitation and mechanistic understanding of MOBs or MOB cells from a synthetic biological approach, providing the novel means for one-pot heterologous protein production with methane, the high-

throughput screening tool for active MOBs, and the insights into non-enzymatic oxidation of methane, a pitfall-artifact that must be considered in future studies.

Chapter III

Methanol production from sugar compounds by synthetic reversed methylotrophy constructed in *Escherichia coli*

Introduction

In bioindustry, methanol is not only a carbon source for microbial fermentation processes, but also a substrate for biological production of industrial chemicals (Ochsner et al. 2015; Schrader et al. 2009; Trotsenko and Torgonskaya 2018). To date, a variety of methods for methanol production via chemical processes have been developed (Olah et al. 2009), however, no biological production processes for methanol from biomass constituents such as sugar compounds, that is analogous to bioethanol production, are currently available. To enable the production of methanol in this manner, construction of a synthetic biological pathway in a heterologous host using enzymes involved in the metabolism of C1 compounds including methanol can be a possible solution.

Methylotrophic bacteria, which can use methanol as the sole carbon and energy source, have diverse types of methanol metabolic pathways. Methanol is first oxidized to formaldehyde by MDHs. Gram-negative methylotrophic bacteria possess MDHs that require pyrroloquinoline quinone (PQQ) as a cofactor (Keltjens et al. 2014). In contrast, gram-positive methylotrophic bacteria possess $NAD(P)^+$-dependent MDHs (Hektor et al. 2000). For example, the thermophilic methylotroph *B. methanolicus* possesses an NAD^+-dependent MDH and this type of MDH requires the activator protein Act for efficient methanol oxidation *in vitro* (Arfman et al. 2004).

Formaldehyde produced by MDH next undergoes further oxidation to CO_2 or fixation

to cell constituents. The two major assimilatory pathways in methylotrophic bacteria are the serine pathway and the ribulose monophosphate (RuMP) pathway (Chistoserdova 2011). In the bacteria which use serine pathway for formaldehyde assimilation, incorporation of a C1 unit into serine involves tetrahydromethanopterin (H_4MPT)- and glutathione-dependent oxidation of formaldehyde to formate, the conjugation of formate and tetrahydrofolate (H_4F) to produce 5,10-methylene-H_4F, and transfer of C1 unit on 5,10-methylene-H_4F to glycine. On the other hand, in the RuMP pathway, formaldehyde is fixed to ribulose 5-phosphate (Ru5P) by 3-hexulose-6-phosphate synthase (HPS), forming D-*arabino*-3-hexulose 6-phosphate (Hu6P), which is then isomerized to F6P by 6-phospho-3-hexuloisomerase (PHI) (Orita et al. 2006).

Recent studies have engineered model bacterium including *E. coli* to incorporate methanol by introducing the enzymes for C1 metabolism (Müller et al. 2015; Meyer et al. 2018; Tuyishime et al. 2018; Witthoff et al. 2015; Woolston et al. 2018; Woolston et al. 2017). These studies have usually employed NAD^+-dependent MDH, HPS and PHI for their ease of functional production in the host species, because these enzymes do not require any methylotrophy-specific cofactors (PQQ, H_4MPT and H_4F), and the substrate Ru5P and the product F6P exist in almost all organisms, enabling coupling to the endogenous pentose phosphate pathway.

Theoretically, the reverse reactions of methanol oxidation and formaldehyde fixation by MDH, HPS and PHI should result in production of methanol from F6P, which can be derived from sugar compounds (Fig. 3-1). In fact, NAD^+-dependent MDH was reported to catalyze the reverse reaction (i.e., reduction of formaldehyde to methanol), which does not require the activator protein Act (Arfman et al. 1989), and the fused form of HPS and PHI (HPS-PHI) found in some hyperthermophilic archaea also catalyzes the reverse reaction (i.e., production of formaldehyde and Ru5P from F6P) (Kato et al. 2006; Orita et al. 2006). Here I describe the construction of a reversed methylotrophic pathway to produce methanol from F6P or glucose

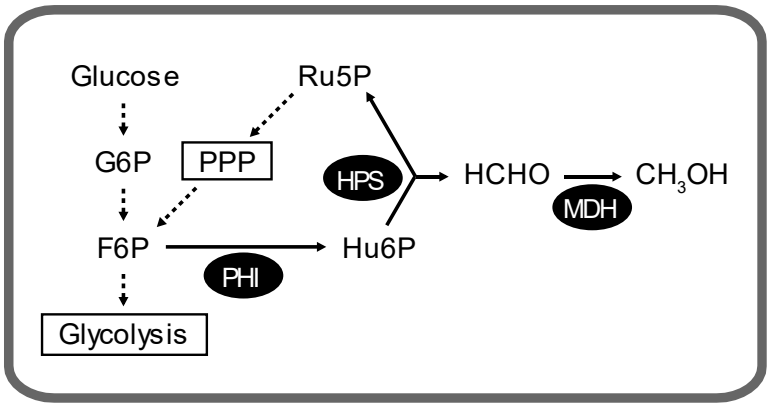

Fig. 3-1 Schematic diagram of the reversed methylotrophic pathway to produce methanol from F6P or glucose in recombinant *E. coli* cells. Solid arrows indicate reverse reactions of methanol oxidation and formaldehyde fixation via MDH and the RuMP pathway, respectively. Dashed arrows indicate endogenous metabolic pathways in *E. coli*. G6P, glucose 6-phosphate; F6P, fructose 6-phosphate; Ru5P, ribulose 5-phosphate; Hu6P, D-arabino-3-hexulose 6-phosphate; HPS, 3-hexulose-6-phosphate synthase; PHI, 6-phospho-3-hexuloisomerase; MDH, methanol dehydrogenase; PPP, non-oxidative pentose phosphate pathway.

in engineered *E. coli* cells that express genes encoding NAD^+-dependent MDH from *B. methanolicus* S1 (Arfman et al. 1992; Yurimoto et al. 2002), and the artificial fusion enzyme HPS-PHI, which was constructed with the *hps* and *phi* genes from *M. gastri* MB19 (Orita et al. 2007). To my knowledge, this would be the first report of the biotechnological use of the reverse reactions of C1 metabolism, and these results provide a starting point towards the industrially relevant biological supply of methanol from biomass-derived sugars.

Materials and methods

Strains and culture conditions

E. coli strains used in this study are listed in Table 3-1. *E. coli* transformants were grown in LB medium at 37°C, to which 0.5 mM isopropyl-β-D-thiogalactopyranoside (IPTG) was added at mid-exponential phase (OD_{610} of 0.4-0.6), followed by overnight growth at 16°C to achieve an OD_{610} of 2-3. Ampicillin (50 μg/mL) and chloramphenicol (30 μg/mL) were added when applicable.

Plasmid construction

Plasmids used in this study are listed in Table 3-2. Oligonucleotide primers used in this study are listed in Table 3-3. The 1.1-kb *mdh* gene from *B. methanolicus* S1 excluding the stop codon was amplified by PCR from the genomic DNA. The 5'-end of each primer contained NheI or HindIII sites. This PCR product and the EcoRV-digested pBluescript II SK(+) were ligated to

Table 3-1 *E. coli* strains used in this study

E. coli strain	Description	Source or reference
Rosetta (DE3)	F^- *ompT hsdS*$_B$($r_B^-m_B^-$) *gal dcm*(DE3) pRARE (Cam^R)	Novagen
Rosetta (DE3) [pET-23a(+)]	Rosetta (DE3) harboring pET-23a(+)	This study
Rosetta (DE3) [pETmdh-His]	Rosetta (DE3) harboring pETmdh-His	This study
Rosetta (DE3) [pEThps-phi]	Rosetta (DE3) harboring pEThps-phi	Orita et al. (2007)
Rosetta (DE3) [pETDuet]	Rosetta (DE3) harboring pETDuet-1	This study
Rosetta (DE3) [pDmHhp]	Rosetta (DE3) harboring pDmHhp	This study

Table 3-2 Plasmids used in this study

Plasmid	Description	Source or reference
pBluescript II SK(+)	Cloning vector	Stratagene
pBSmdh	pBluescript II SK(+) derivative; *mdh* from *B. methanolicus* S1 without the stop codon	This study
pET-23a(+)	T7 promoter-based expression vector	Novagen
pETmdh-His	pET-23a(+) derivative; *mdh* from *B. methanolicus* S1 in frame with C-terminal 6×His-tag	This study
pEThps-phi	pET-23a(+) derivative; *hps-phi*	Orita et al. (2007)
pETDuet-1	T7 promoter-based expression vector for two genes	Novagen
pDmH	pETDuet-1 derivative; *mdh*-His_6 from pETmdh-His in one of the two multiple cloning sites	This study
pDmHhp	pDmH derivative; *hps-phi* in the other multiple cloning site	This study

Table 3-3 Oligonucleotide primers used in this study

Primer	Sequence (5'-3')	Purpose
mdh-fw-NheI	CTAGCTAGCATGACAAACTTTTTCATTCC	Amplification of *mdh* gene excluding the stop codon from the genomic DNA of *B. methanolicus* S1 for construction of pBSmdh
mdh-rv-HindIII(Histag)	CCCAAGCTTCAGAGCGTTTTTGATGATTT	
mdh-fw-NcoI	CATGCCATGGGCATGACAAACTTTTTCATTCC	Amplification of *mdh*-His_6 from pETmdh-His for construction of pDmH
mdh-His-rv-EcoRI	GGAATTCTCAGTGGTGGTGGTGGTGGTGCT	
MhMp-BglII	GAAGATCTCATGAAGCTCCAAGTCTCCAT	Amplification of *hps-phi* from pEThps-phi for construction of pDmHhp
MhMp-KpnI	GGGGTACCTCACTCGAGGTTGGCGTGGCGCG	

obtain pBSmdh. pETmdh-His was constructed by ligating the 1.1- and 3.6-kb NheI/HindIII fragments of pBSmdh and pET-23a(+). pDmH was constructed by inserting *mdh*-His_6 from pETmdh-His into the NcoI/EcoRI sites of pETDuet-1. pDmHhp was constructed by inserting *hps-phi* from pEThps-phi (Orita et al. 2007) into the BglII/KpnI sites of pDmH. The expression vectors were introduced into *E. coli* Rosetta (DE3) by electroporation.

Preparation of cell-free extract

For purification of recombinant *B. methanolicus* S1 MDH tagged with 6xHis, IPTG-induced *E. coli* [pETmdh-His] cells were suspended in buffer A (50 mM potassium phosphate buffer (KPB, pH 7.5), 5 mM $MgSO_4$ and 1 mM dithiothreitol (DTT)) and then disrupted by French press (Constant cell disruption system one shot model, Constant Systems Ltd., UK). After centrifugation at 5,000 × *g* for 30 min at 4°C, the resulting supernatant was used as a cell-free extract. For preparation of a cell-free extract of IPTG-induced *E. coli* [pEThps-phi], and *E. coli* [pDmHhp], cells were suspended in buffer B (50 mM KPB (pH 6.5), 1 mM DTT, 0.1 mM phenylmethylsulfonyl fluoride (PMSF) and 5 mM $MgCl_2$), and disrupted by French press. After centrifugation at 10,000 × *g* for 10 min at 4°C, resulting supernatant was used as a cell-free extract.

Purification of recombinant *B. methanolicus* S1 MDH tagged with 6xHis

Cell-free extract (7.5 mL) was loaded onto 2 mL of column-packed Ni-NTA Agarose (QIAGEN, Hilden, Germany) preequilibrated with buffer C (57.5 mM NaH_2PO_4, 300 mM NaCl, pH adjusted to 8.0 with NaOH) containing 10 mM imidazole. The column was then washed twice with 2 column volumes of buffer C containing 20 mM imidazole. The column-bound protein was eluted with 2 mL of buffer C containing 250 mM imidazole. The eluted fraction was dialyzed against 50 mM KPB (pH 7.5) and used as purified MDH-His_6.

Protein analyses

Protein concentrations were determined using a Bio-Rad protein assay kit (Bio-Rad) with bovine serum albumin as the standard (Bradford 1976). For SDS-PAGE, protein samples (10 μg) were mixed with 3× sample buffer (see "Materials and methods" section of Section I of Chapter II), boiled for 5 min and run on a 12% gel. For total protein staining, GelCode^{TM} Blue Safe Protein Stain (Thermo Scientific, Waltham, MA) was used. For immunoblot analyses, proteins were transferred onto a PVDF membrane by semidry blotting (Bio-Rad). 6×His-tagged proteins were detected using anti-His-tag mAb-HRP-DirecT (Medical & Biological Laboratories) at a 1:5,000 dilution and Western Lightning (Perkin-Elmer Life Science). HPS-PHI proteins were detected using rabbit anti-HPS antibody as described previously (Orita et al. 2007). The signal was analyzed with LuminoGraph II (ATTO).

Enzyme assay

Formaldehyde reductase (FRD) activity was determined by following the formaldehyde-dependent oxidation of NADH as described previously (Arfman et al. 1989). The K_m and k_{cat} values of purified MDH-His_6 were determined using a Lineweaver-Burk plot of initial reaction velocity against different concentrations of the substrate formaldehyde. The activity of HPS-PHI to catalyze the forward reaction (F6P synthesis) was determined by following the Ru5P-dependent production of F6P as described previously (Orita et al. 2007) except that the formaldehyde and ribose 5-phosphate concentrations were 2.5 mM. The activity of HPS-PHI to catalyze the reverse reaction (formaldehyde production) was determined by following the F6P-dependent production of formaldehyde as described previously (Orita et al. 2006) except that the reaction was performed at 30°C. One unit of activity was defined as the amount of enzyme that oxidized 1 μmol of NADH (FRD reaction), produced 1 μmol of F6P (HPS-PHI forward reaction), or produced 1 μmol of formaldehyde (HPS-PHI reverse reaction) per min.

Each activity value is presented as mean ± standard deviation of triplicate measurements.

Production of methanol by whole-cell reaction

For production of methanol from formaldehyde, IPTG-induced *E. coli* [pETmdh-His] and *E. coli* [pET-23a(+)] cells were suspended in 50 mM KPB (pH 6.7), 5 mM $MgSO_4$, 1 mM DTT and 10 mM formaldehyde, to achieve an OD_{610} of 2.0, and incubated at 37°C. For production of methanol from F6P, IPTG-induced cells of *E. coli* [pDmHhp], *E. coli* [pETDuet], or mixture of *E. coli* [pETmdh-His] and *E. coli* [pEThps-phi] were suspended in 100 mM KPB (pH 6.5), 5 mM $MgCl_2$ and 100 mM F6P, to achieve an OD_{610} of 8.0, and incubated at 37°C. Methanol contained in the purchased F6P (Sigma-Aldrich Japan K.K., Tokyo, Japan) was removed in advance by dissolving F6P in 70% (v/v) acetonitrile and removing the solvent by a centrifugal evaporator. For production of methanol from glucose, IPTG-induced *E. coli* [pDmHhp] and *E. coli* [pETDuet] cells were suspended in 100 mM KPB (pH 6.5), 5 mM $MgCl_2$ and 2% (w/v) glucose, to achieve an OD_{610} of 10, and incubated at 37°C. In these experiments, the reaction volume was 1 mL, and at each time point, 0.1 mL was sampled, centrifuged at 20,000 × *g* for 2 min at 4°C, and the resulting supernatant was stored at 4°C. The methanol concentration in the supernatant was determined using a GC-2014 (Shimadzu) gas chromatograph equipped with a flame ionization detector and DB-1 column (30 m × 0.25 mm i.d. × 0.25 μm, Agilent Technologies, Santa Clara, CA, USA). Nitrogen gas was used as the carrier. The temperature program of the oven was 40°C for 5 min, then a ramp of 20°C min^{-1} to 200°C (held for 15 min), and the injector and detector were set at 250°C.

Results

Recombinant *B. methanolicus* S1 MDH catalyzes NADH-dependent reduction of formaldehyde to methanol both *in vitro* and *in vivo*

To confirm that recombinant MDH from *B. methanolicus* S1 catalyzes NADH-dependent reduction of formaldehyde to methanol as reported for the enzyme from *B. methanolicus* C1 (Arfman et al. 1989), I constructed a T7 promoter-based expression vector for the NAD^+-dependent MDH gene (*mdh*) from *B. methanolicus* S1 tagged with 6×His and introduced it into *E. coli* Rosetta (DE3). Although efficient methanol oxidation by the NAD^+-dependent MDH requires the activator protein Act, I did not express it because it is not required for the reverse reaction (Arfman et al. 1991; Arfman et al. 1989). After production in *E. coli*, I purified MDH-His_6 using the Ni-NTA column (Fig. 3-2). The specific activity of the purified MDH-His_6 to reduce formaldehyde to methanol with NADH was 10.0 units/mg at 37°C. This value was

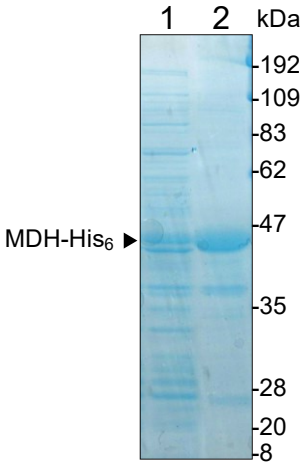

Fig. 3-2 SDS-PAGE analysis of the protein production and purification of recombinant MDH tagged with 6×His (MDH-His_6) using a Ni-NTA column. Lane 1, Cell-free extract of *E. coli* [pETmdh-His]. Lane 2, Imidazole elution of MDH-His_6 from the Ni-NTA column. The theoretical molecular mass of MDH-His_6 is 42 kDa.

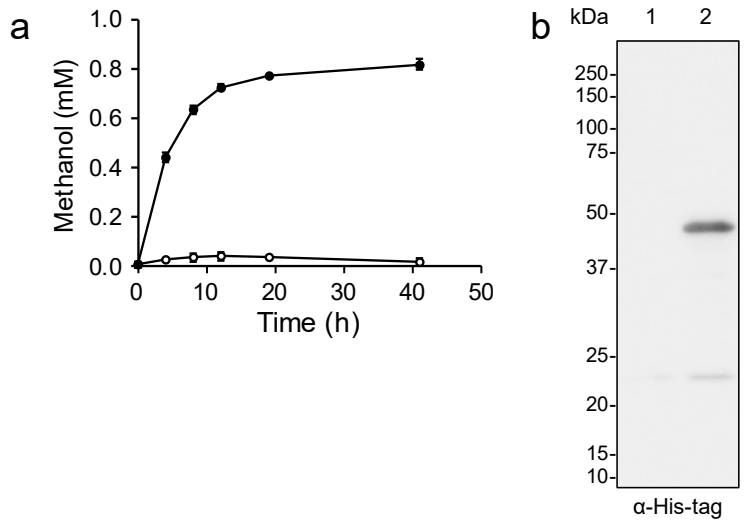

Fig. 3-3 Production of methanol from formaldehyde in a whole-cell reaction of *E. coli* expressing *mdh*-His$_6$. **a** IPTG-induced *E. coli* [pET-23a(+)] (open circles) and *E. coli* [pETmdh-His] (closed circles) cells were suspended in a reaction mixture containing 10 mM formaldehyde and incubated at 37°C for the indicated time. The methanol concentration in the supernatant was determined by gas chromatography (GC). The means ± standard deviations of triplicate incubations are shown. FRD activity of the cell-free extracts of *E. coli* [pET-23a(+)] and *E. coli* [pETmdh-His] cells used in this experiment were not detected and $(1.3 \pm 0.1) \times 10^{-2}$ units/mg at 37°C, respectively. **b** Immunoblot analysis of MDH-His$_6$ protein in the cell-free extracts of the cells used in **a**. Lane 1, *E. coli* [pET-23a(+)]. Lane 2, *E. coli* [pETmdh-His]. The size of the major band appeared in lane 2 (42 kDa) agreed with that in lane 2 of Fig. 3-2, confirming the production of MDH-His$_6$ protein in the *E. coli* [pETmdh-His] cells.

comparable to that of MDH purified from *B. methanolicus* C1 (19.6 units/mg at 50°C) (Arfman et al. 1989) or the recombinant *E. coli* strain expressing the MDH gene of strain C1 (3.5 units/mg at 50°C) (de Vries et al. 1992). K_m and k_{cat} values for my purified MDH-His$_6$ at 37°C were 2.1 mM and 6.8 s^{-1}, respectively. Taken together, recombinant MDH from *B. methanolicus* S1 can catalyze NADH-dependent reduction of formaldehyde to methanol *in vitro*.

Next, I tested whether *E. coli* cells expressing MDH-His$_6$ can produce methanol from formaldehyde in whole-cell reactions. After induction of *mdh*-His$_6$ by IPTG, *E. coli* [pETmdh-

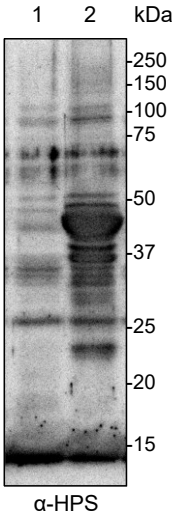

Fig. 3-4 Immunoblot analysis of HPS-PHI protein in the cell-free extracts of *E. coli* [pET-23a(+)] (lane 1) and *E. coli* [pEThps-phi] (lane 2) cells. The size of the major band appeared in lane 2 (42 kDa) agreed with that of purified HPS-PHI observed previously (Orita et al. 2007), confirming the production of HPS-PHI protein in the *E. coli* [pEThps-phi] cells.

His] cells were incubated in buffer containing 10 mM formaldehyde at 37°C. As a result, I observed an increase in the methanol concentration in the reaction mixture, which was not observed with cells harboring empty vector (*E. coli* [pET-23a(+)]) (Fig. 3-3a). Therefore, *E. coli* cells producing recombinant MDH from *B. methanolicus* S1 can produce methanol from formaldehyde. The methanol concentration after 41 h of incubation was 0.82 ± 0.02 mM. In this experiment, the production of MDH-His_6 protein was confirmed by immunoblot analysis (Fig. 3-3b).

Artificial fusion protein HPS-PHI catalyzes production of formaldehyde from F6P

I next investigated whether the artificial fusion enzyme HPS-PHI derived from *M. gastri* MB19 (Orita et al. 2007) catalyzes formaldehyde production from F6P. I used *E. coli* [pEThps-phi] for production of the enzyme. Cell-free extract of IPTG-induced *E. coli* [pEThps-phi] cells was

prepared and subjected to enzyme assays. The specific activities for forward (F6P production) and reverse (formaldehyde production) reactions were 2.0 ± 0.6 and (6.1 ± 0.1) × 10^{-1} units/mg, respectively. Neither enzyme activity was detected with cells harboring empty vector (*E. coli* [pET-23a(+)]). The production of HPS-PHI protein was confirmed by immunoblot analysis (Fig. 3-4). Therefore, it was confirmed that the artificial HPS-PHI can catalyze both the forward and reverse reactions as reported for HPS-PHI from hyperthermophilic archaea (Kato et al. 2006; Orita et al. 2006).

Production of methanol from F6P through sequential reactions catalyzed by HPS-PHI and MDH

To test whether methanol can be produced from F6P through the sequential reactions catalyzed by HPS-PHI and MDH, I constructed a plasmid vector for co-expression of the genes encoding MDH-His_6 and HPS-PHI (pDmHhp), and introduced it into *E. coli* Rosetta (DE3). To confirm the co-expression of these genes, the cell-free extract of IPTG-induced *E. coli* [pDmHhp] cells was subjected to enzyme assays. Specific activities for formaldehyde reduction catalyzed by MDH at 37°C and for formaldehyde fixation catalyzed by HPS-PHI at 30°C were (3.4 ± 0.5) × 10^{-2} and (5.3 ± 0.3) × 10^{-1} units/mg, respectively. Neither enzyme activity was detected with cells harboring empty vector (*E. coli* [pETDuet]). The co-production of MDH-His_6 and HPS-PHI proteins was confirmed by immunoblot analyses (Fig. 3-5a). Thus, I succeeded in co-expressing genes encoding these two enzymes. Next, I tested whether cells expressing *mdh*-His_6 and *hps-phi* can produce methanol from F6P in resting cell reactions. IPTG-induced *E. coli* [pDmHhp] cells were incubated in buffer containing 100 mM F6P for 24 h at 37°C. Results showed that methanol accumulated up to 1.5 ± 0.1 mM in the reaction mixture (Fig. 3-5b), which was not observed for *E. coli* [pETDuet] cells (Fig. 3-5b) or in the absence of F6P (data not shown). Thus, *E. coli* cells co-expressing *mdh*-His_6 and *hps-phi* could produce methanol

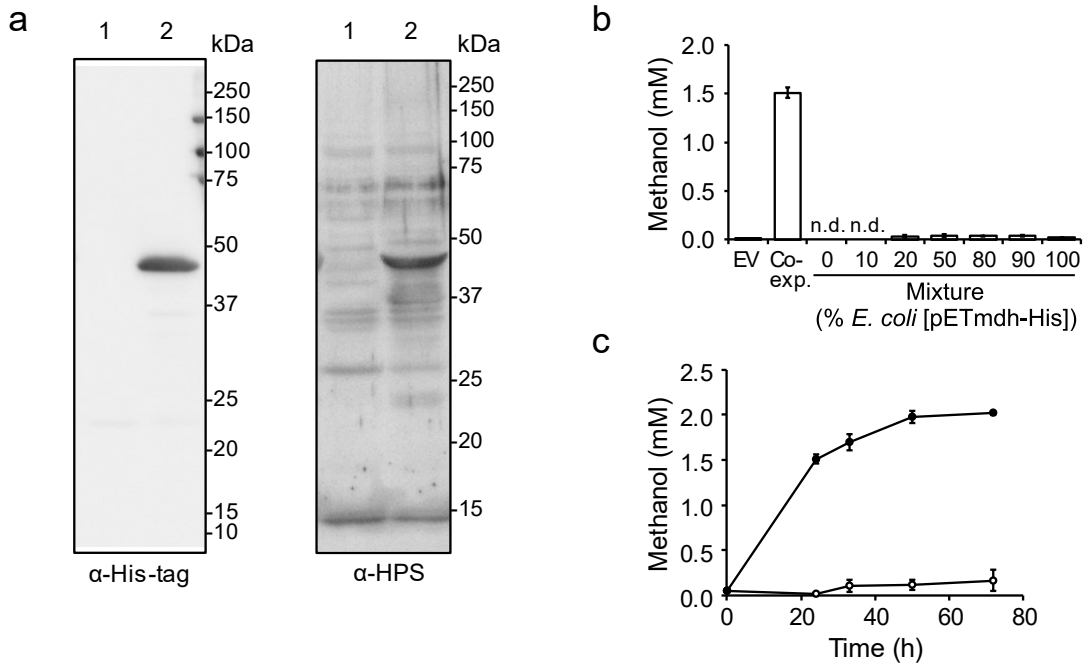

Fig. 3-5 Production of methanol from F6P in whole-cell reactions of *E. coli* expressing *mdh*-His$_6$ and *hps-phi*. **a** Immunoblot analyses of MDH-His$_6$ and HPS-PHI proteins in the cell-free extracts of *E. coli* [pETDuet] (lane 1) and *E. coli* [pDmHhp] (lane 2) cells. The sizes of the major bands appeared in lane 2 in α-His-tag and α-HPS-detections agreed with that of Fig. 3-3b and 3-4, respectively, confirming the co-production of MDH-His$_6$ and HPS-PHI proteins. **b** Methanol production by *E. coli* [pETDuet] cells (EV), *E. coli* [pDmHhp] cells (co-exp.) or the mixtures of *E. coli* [pETmdh-His] and *E. coli* [pEThps-phi] cells at different ratios. IPTG-induced cells were suspended in a reaction mixture containing 100 mM F6P and incubated at 37°C for 24 h. n.d., not determined. **c** Time-course of methanol production by *E. coli* [pETDuet] cells (open circles) and *E. coli* [pDmHhp] (closed circles). Reaction conditions and the analytical method were the same as in **b**, and the cells were incubated for the indicated time. The means ± standard deviations of triplicate incubations are shown.

from F6P. On the other hand, 20 ± 3 μM methanol was detected with *E. coli* [pETmdh-His] cells alone (Fig. 3-5b, 100% *E. coli* [pETmdh-His]). Nevertheless, the amount of methanol was about 75-fold lower than that by the co-expressing cells. In addition, methanol was not detected with *E. coli* [pEThps-phi] cells (Fig. 3-5b, 0% *E. coli* [pETmdh-His]). Collectively, efficient production of methanol was confirmed to require both MDH-His$_6$ and HPS-PHI. I also tested

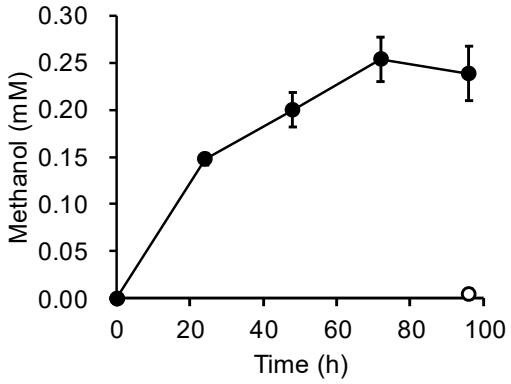

Fig. 3-6 Production of methanol from glucose by *E. coli* expressing *mdh*-His_6 and *hps-phi*. IPTG-induced *E. coli* [pETDuet] (open circles) and *E. coli* [pDmHhp] (closed circles) cells were suspended in the buffer containing 2% (w/v) glucose to an OD_{610} of 10, and incubated at 37°C for the indicated time. The means ± standard deviations of triplicate incubations are shown. For the samples with the *E. coli* [pETDuet] cells before 96 h, the concentrations of methanol were not determined.

the mixture of *E. coli* [pETmdh-His] and *E. coli* [pEThps-phi] cells, expecting that methanol could be produced by *E. coli* [pETmdh-His] cells from formaldehyde produced by *E. coli* [pEThps-phi] cells. However, the amount of methanol produced was less than that with the co-expressing cells with all of the mixing ratios tested (Fig. 3-5b). This result shows that both enzymes should be produced in the same cell for efficient methanol production. This may be because formaldehyde was converted to methanol before formaldehyde induced the endogenous glutathione-dependent formaldehyde oxidation pathway in the co-expressing cells (Gonzalez et al. 2006; Gutheil et al. 1992). With *E. coli* [pDmHhp] cells, the methanol concentration reached 2.0 ± 0.01 mM after 72 h of incubation (Fig. 3-5c).

Production of methanol from glucose by *E. coli* expressing *mdh* and *hps-phi*

Finally, I tested whether glucose could serve as a substrate for methanol production. Theoretically, glucose incorporated into *E. coli* cells is metabolized in glycolysis, producing as

an intermediate F6P, the substrate for methanol production by MDH and HPS-PHI. I suspended *E. coli* [pDmHhp] cells in buffer containing 2% (w/v) glucose, and incubated them at 37°C. I observed accumulation of methanol that was not observed with the *E. coli* [pETDuet] cells (Fig. 3-6). With the *E. coli* [pDmHhp] cells, methanol accumulated up to 0.25 ± 0.02 mM after 72 h of incubation. As described above, methanol was not produced in the absence of substrate. Taken together, methanol was produced from glucose by the catalytic activity of two heterologous enzymes.

Discussion

In this chapter, I established a novel pathway to produce methanol from F6P or glucose in *E. coli* cells via "reversed methylotrophy" by co-expression of genes encoding an NAD^+-dependent MDH and an artificial fusion protein HPS-PHI. These enzymes have been used to confer synthetic methylotrophy to non-methylotrophic microorganisms (Müller et al. 2015; Meyer et al. 2018; Tuyishime et al. 2018; Witthoff et al. 2015; Woolston et al. 2018; Woolston et al. 2017). In this study, I confirmed that these enzymes can catalyze the reverse reactions of C1 metabolism both *in vitro* and *in vivo*, and successfully conferred reversed methylotrophy to *E. coli* (Fig. 3-1).

The molar yield of methanol from formaldehyde by *E. coli* expressing *mdh* was 8.2% (Fig. 3-3). Methanol was likely to have accumulated due to the absence of the MDH activator protein Act, which accelerates the undesired methanol oxidation reaction. Better yield may be achieved by eliminating the endogenous formaldehyde detoxification pathway (Gonzalez et al. 2006; Gutheil et al. 1992). Next, the molar yield of methanol from F6P by *E. coli* co-expressing *mdh* and *hps-phi* was 2.0% (Fig. 3-5c). This low yield can be ascribed to low expression level of the endogenous sugar phosphate-uptake system (Weston and Kadner 1988) or inactivation of MDH-His_6 and HPS-PHI, whose expression was not induced during the incubation with F6P. Finally, the molar yield of methanol from glucose was 0.23% (Fig. 3-6), which was less than that from F6P. The yield may be improved by promoting glucose incorporation or engineering sugar metabolism to increase intracellular concentration of F6P, the substrate for methanol production by MDH and HPS-PHI. In this study, I did not attempt the production of methanol during growth on glucose because I adopted the pET vector system, whose promotor for the gene of interest is repressed in the presence of glucose. The use of a glucose non-repressible promoter will be suitable for methanol production accompanied by the growth on glucose. In

spite of the low yield of methanol from glucose, I succeeded in endogenous supply of methanol within the host cells, which has the potential to be utilized for bioproduction of useful compounds that need a methoxy group donor. For example, methanol supply is necessary for alcohol acyltransferase-catalyzed production of methyl short-chain esters (methyl acrylate, methyl methacrylate, and other methylester derivatives), which can be used as solvent, plasticizer or lubricant (Kruis et al. 2019). In such situations, methanol is usually supplied exogenously, however, introducing an endogenous production pathway for methanol and its use as the enzyme substrate within host cells would obviate the need for the exogenous supply and simplify the production process.

Because F6P is a ubiquitous metabolic intermediate, the substrate for methanol production can be expanded to other biomass-derived sugars, photosynthetic products, etc. Therefore, this work provides a versatile concept for the biological production and intracellular supply of methanol from various types of substrates that is useful for production of industrial chemicals including methylesters. Furthermore, this concept is expected to be extended to bioindustrial production of methanol, a promising feedstock, from biomass.

Conclusion

In this study, I described the synthetic biological studies on production of methanol from natural resource-derived carbon compounds.

In Chapter I, I developed the methanol-biosensing technology with the methylotrophic yeast *K. phaffii* and its single-cell analyses. Selection of the promoter, optimization of preculture and sensing conditions, and FACS analysis of the distribution of cellular fluorescence intensity improved the limit of detection for methanol to the micromolar range.

In Chapter II, I conducted single-cell visualization of methanol-producing enzyme activities with the *K. phaffii* methanol sensor. In Section I, I introduced heterologous *A. niger* PME gene expression cassettes into the methanol sensor yeast cells, and succeeded in visualization of the activity of the produced PME, whose activity at a single-cell level varied among the strains. Through this analysis, I proved the concept of the high-throughput selection of the single methanol sensor cell having high methanol-producing enzyme activity with FACS. This concept would strongly facilitate the development of microbial cells or engineered enzymes having high methanol-producing activities.

In Section II, I visualized the methane oxidation activity with *Mycolicibacterium* sp. TY-6 cell reaction. In the co-culture with *Mycolicibacterium* sp. TY-6 cells in the presence of methane, the *K. phaffii* methanol sensor cells produced the fluorescent protein Venus-PTS1 with the methanol produced from methane by *Mycolicibacterium* sp. TY-6 cells. From this result, I demonstrated the use of the methanol sensor cells for detection of methanol produced by MOBs, and the one-pot synthesis of heterologous proteins from methane in this co-culture. In addition, I confirmed that non-enzymatic oxidation of methane to methanol was caused by duroquinol or H_2O_2. These findings will aid future engineering and analysis of MOBs.

In Chapter III, I constructed the synthetic reversed methylotrophic pathway that

produced methanol from F6P or glucose by engineering *E. coli* cells to express NAD^+-dependent MDH from *B. methanolicus* S1 and the artificial *M. gastri* MB19 HPS-PHI. This technology provides the novel means for production of methanol from various biomass-derived sugar compounds.

References

Abanda-Nkpwatt D, Müsch M, Tschiersch J, Boettner M, Schwab W (2006) Molecular interaction between *Methylobacterium extorquens* and seedlings: growth promotion, methanol consumption, and localization of the methanol emission site. J Exp Bot 57:4025-4032. https://doi.org/10.1093/jxb/erl173

Ahmad M, Hirz M, Pichler H, Schwab H (2014) Protein expression in *Pichia pastoris*: recent achievements and perspectives for heterologous protein production. Appl Microbiol Biotechnol 98:5301-5317. https://doi.org/10.1007/s00253-014-5732-5

Anthon GE, Barrett DM (2004) Comparison of three colorimetric reagents in the determination of methanol with alcohol oxidase. Application to the assay of pectin methylesterase. J Agric Food Chem 52:3749-3753. https://doi.org/10.1021/jf035284w

Arfman N, Dijkhuizen L, Kirchhof G, Ludwig W, Schleifer K-H, Bulygina ES, Chumakov KM, Govorukhina NI, Trotsenko YA, White D, Sharp RJ (1992) *Bacillus methanolicus* sp. nov., a new species of thermotolerant, methanol-utilizing, endospore-forming bacteria. Int J Syst Evol Microbiol 42:439-445. https://doi.org/10.1099/00207713-42-3-439

Arfman N, Hektor HJ, Bystrykh LV, Govorukhina NI, Dijkhuizen L, Frank J (2004) Properties of an NAD(H)-containing methanol dehydrogenase and its activator protein from *Bacillus methanolicus*. Eur J Biochem 244:426-433. https://doi.org/10.1111/j.1432-1033.1997.00426.x

Arfman N, Van Beeumen J, De Vries GE, Harder W, Dijkhuizen L (1991) Purification and characterization of an activator protein for methanol dehydrogenase from thermotolerant *Bacillus* spp. J Biol Chem 266:3955-3960.

Arfman N, Watling EM, Clement W, van Oosterwijk RJ, de Vries GE, Harder W, Attwood MM, Dijkhuizen L (1989) Methanol metabolism in thermotolerant methylotrophic *Bacillus*

strains involving a novel catabolic NAD-dependent methanol dehydrogenase as a key enzyme. Arch Microbiol 152:280-288. https://doi.org/10.1007/BF00409664

Balasubramanian R, Smith SM, Rawat S, Yatsunyk LA, Stemmler TL, Rosenzweig AC (2010) Oxidation of methane by a biological dicopper centre. Nature 465:115-119. https://doi.org/10.1038/nature08992

Bradford MM (1976) A rapid and sensitive method for the quantitation of microgram quantities of protein utilizing the principle of protein-dye binding. Anal Biochem 72:248-254. https://doi.org/10.1016/0003-2697(76)90527-3

Chan SI, Lee SJ (2019) The biochemistry of methane monooxygenases. Methanotrophs: microbiology fundamentals and biotechnological applications. Springer International Publishing, Cham, pp 71-120. https://doi.org/10.1007/978-3-030-23261-0_3

Chistoserdova L (2011) Modularity of methylotrophy, revisited. Environ Microbiol 13:2603-2622. https://doi.org/10.1111/j.1462-2920.2011.02464.x

Clomburg JM, Crumbley AM, Gonzalez R (2017) Industrial biomanufacturing: The future of chemical production. Science 355:aag0804. https://doi.org/10.1126/science.aag0804

Davis RW, Thomas M, Cameron J, St. John TP, Scherer S, Padgett RA (1980) Rapid DNA isolations for enzymatic and hybridization analysis. Methods Enzymol. vol 65. Academic Press, pp 404-411. https://doi.org/10.1016/S0076-6879(80)65051-4

de Vries GE, Arfman N, Terpstra P, Dijkhuizen L (1992) Cloning, expression, and sequence analysis of the *Bacillus methanolicus* C1 methanol dehydrogenase gene. J Bacteriol 174:5346-5353. https://doi.org/10.1128/jb.174.16.5346-5353.1992

DeLoache WC, Russ ZN, Narcross L, Gonzales AM, Martin VJ, Dueber JE (2015) An enzyme-coupled biosensor enables (*S*)-reticuline production in yeast from glucose. Nat Chem Biol 11:465-471. https://doi.org/10.1038/nchembio.1816

Gellissen G (2000) Heterologous protein production in methylotrophic yeasts. Appl Microbiol

Biotechnol 54:741-750. https://doi.org/10.1007/s002530000464

Gonzalez CF, Proudfoot M, Brown G, Korniyenko Y, Mori H, Savchenko AV, Yakunin AF (2006) Molecular basis of formaldehyde detoxification. Characterization of two *S*-formylglutathione hydrolases from *Escherichia coli*, FrmB and YeiG. J Biol Chem 281:14514-14522. https://doi.org/10.1074/jbc.M600996200

Gould SJ, McCollum D, Spong AP, Heyman JA, Subramani S (1992) Development of the yeast *Pichia pastoris* as a model organism for a genetic and molecular analysis of peroxisome assembly. Yeast 8:613-628. https://doi.org/10.1002/yea.320080805

Guilbault GG, Danielsson B, Mandenius CF, Mosbach K (1983) Enzyme electrode and thermistor probes for determination of alcohols with alcohol oxidase. Anal Chem 55:1582-1585.

Gutheil WG, Holmquist B, Vallee BL (1992) Purification, characterization, and partial sequence of the glutathione-dependent formaldehyde dehydrogenase from *Escherichia coli*: a class III alcohol dehydrogenase. Biochemistry 31:475-481. https://doi.org/10.1021/bi00117a025

Hektor HJ, Kloosterman H, Dijkhuizen L (2000) Nicotinoprotein methanol dehydrogenase enzymes in Gram-positive methylotrophic bacteria. J Mol Catal B: Enzym 8:103-109. https://doi.org/10.1016/S1381-1177(99)00073-9

Ho JCH, Pawar SV, Hallam SJ, Yadav VG (2018) An improved whole-cell biosensor for the discovery of lignin-transforming enzymes in functional metagenomic screens. ACS Synth Biol 7:392-398. https://doi.org/10.1021/acssynbio.7b00412

Iguchi H, Yurimoto H, Sakai Y (2010) Soluble and particulate methane monooxygenase gene clusters of the type I methanotroph *Methylovulum miyakonense* HT12. FEMS Microbiol Lett 312:71-76. https://doi.org/10.1111/j.1574-6968.2010.02101.x

Iguchi H, Yurimoto H, Sakai Y (2011) *Methylovulum miyakonense* gen. nov., sp. nov., a type I

methanotroph isolated from forest soil. Int J Syst Evol Microbiol 61:810-815. https://doi.org/10.1099/ijs.0.019604-0

Jha RK, Kern TL, Fox DT, CE MS (2014) Engineering an *Acinetobacter* regulon for biosensing and high-throughput enzyme screening in *E. coli* via flow cytometry. Nucleic Acids Res 42:8150-8160. https://doi.org/10.1093/nar/gku444

Kato N, Yurimoto H, Thauer RK (2006) The physiological role of the ribulose monophosphate pathway in bacteria and archaea. Biosci Biotechnol Biochem 70:10-21. https://doi.org/10.1271/bbb.70.10

Kawaguchi K, Yurimoto H, Oku M, Sakai Y (2011) Yeast methylotrophy and autophagy in a methanol-oscillating environment on growing *Arabidopsis thaliana* leaves. PLoS One 6:e25257. https://doi.org/10.1371/journal.pone.0025257

Kawaguchi K, Yurimoto H, Sakai Y (2014) Expression of a codon-optimized *Aspergillus niger* pectin methylesterase gene in the methylotrophic yeast *Candida boidinii*. Biosci Biotechnol Biochem 78:718-721. https://doi.org/10.1080/09168451.2014.891936

Keltjens JT, Pol A, Reimann J, Op den Camp HJM (2014) PQQ-dependent methanol dehydrogenases: rare-earth elements make a difference. Appl Microbiol Biotechnol 98:6163-6183. https://doi.org/10.1007/s00253-014-5766-8

Kim HJ, Huh J, Kwon YW, Park D, Yu Y, Jang YE, Lee B-R, Jo E, Lee EJ, Heo Y, Lee W, Lee J (2019) Biological conversion of methane to methanol through genetic reassembly of native catalytic domains. Nat Catal 2:342-353. https://doi.org/10.1038/s41929-019-0255-1

Kohli P, Kalia M, Gupta R (2015) Pectin methylesterases: a review. J Bioprocess Biotech 5:1. https://doi.org/10.4172/2155-9821.1000227

Kotani T, Kawashima Y, Yurimoto H, Kato N, Sakai Y (2006) Gene structure and regulation of alkane monooxygenases in propane-utilizing *Mycobacterium* sp. TY-6 and

Pseudonocardia sp. TY-7. J Biosci Bioeng 102:184-192. https://doi.org/10.1263/jbb.102.184

Kruis AJ, Bohnenkamp AC, Patinios C, van Nuland YM, Levisson M, Mars AE, van den Berg C, Kengen SWM, Weusthuis RA (2019) Microbial production of short and medium chain esters: Enzymes, pathways, and applications. Biotechnol Adv https://doi.org/10.1016/j.biotechadv.2019.06.006

Liang S, Wang B, Pan L, Ye Y, He M, Han S, Zheng S, Wang X, Lin Y (2012) Comprehensive structural annotation of *Pichia pastoris* transcriptome and the response to various carbon sources using deep paired-end RNA sequencing. BMC Genomics 13:738. https://doi.org/10.1186/1471-2164-13-738

Müller JEN, Meyer F, Litsanov B, Kiefer P, Potthoff E, Heux S, Quax WJ, Wendisch VF, Brautaset T, Portais J-C, Vorholt JA (2015) Engineering *Escherichia coli* for methanol conversion. Metab Eng 28:190-201. https://doi.org/10.1016/j.ymben.2014.12.008

Meyer F, Keller P, Hartl J, Gröninger OG, Kiefer P, Vorholt JA (2018) Methanol-essential growth of *Escherichia coli*. Nat Commun 9:1508. https://doi.org/10.1038/s41467-018-03937-y

Michener JK, Thodey K, Liang JC, Smolke CD (2012) Applications of genetically-encoded biosensors for the construction and control of biosynthetic pathways. Metab Eng 14:212-222. https://doi.org/10.1016/j.ymben.2011.09.004

Mustafi N, Grunberger A, Kohlheyer D, Bott M, Frunzke J (2012) The development and application of a single-cell biosensor for the detection of L-methionine and branched-chain amino acids. Metab Eng 14:449-457. https://doi.org/10.1016/j.ymben.2012.02.002

Nagai T, Ibata K, Park ES, Kubota M, Mikoshiba K, Miyawaki A (2002) A variant of yellow fluorescent protein with fast and efficient maturation for cell-biological applications.

Nat Biotechnol 20:87-90. https://doi.org/10.1038/nbt0102-87

Nakagawa T, Yamada K, Fujimura S, Ito T, Miyaji T, Tomizuka N (2005) Pectin utilization by the methylotrophic yeast *Pichia methanolica*. Microbiology 151:2047-2052. https://doi.org/doi:10.1099/mic.0.27895-0

Ochsner AM, Sonntag F, Buchhaupt M, Schrader J, Vorholt JA (2015) *Methylobacterium extorquens*: methylotrophy and biotechnological applications. Appl Microbiol Biotechnol 99:517-534. https://doi.org/10.1007/s00253-014-6240-3

Ohsawa S, Yurimoto H, Sakai Y (2017) Novel function of Wsc proteins as a methanol-sensing machinery in the yeast *Pichia pastoris*. Mol Microbiol 104:349-363. https://doi.org/10.1111/mmi.13631

Olah GA, Goeppert A, Prakash GS (2009) Beyond oil and gas: the methanol economy, 2nd edn. Wiley-VCH, Weinheim

Orita I, Sakamoto N, Kato N, Yurimoto H, Sakai Y (2007) Bifunctional enzyme fusion of 3-hexulose-6-phosphate synthase and 6-phospho-3-hexuloisomerase. Appl Microbiol Biotechnol 76:439-445. https://doi.org/10.1007/s00253-007-1023-8

Orita I, Sato T, Yurimoto H, Kato N, Atomi H, Imanaka T, Sakai Y (2006) The ribulose monophosphate pathway substitutes for the missing pentose phosphate pathway in the archaeon *Thermococcus kodakaraensis*. J Bacteriol 188:4698-4704. https://doi.org/10.1128/jb.00492-06

Pontes H, Guedes de Pinho P, Casal S, Carmo H, Santos A, Magalhães T, Remião F, Carvalho F, Bastos ML (2009) GC determination of acetone, acetaldehyde, ethanol, and methanol in biological matrices and cell culture. J Chromatogr Sci 47:272-278. https://doi.org/10.1093/chromsci/47.4.272

Ross MO, MacMillan F, Wang J, Nisthal A, Lawton TJ, Olafson BD, Mayo SL, Rosenzweig AC, Hoffman BM (2019) Particulate methane monooxygenase contains only

mononuclear copper centers. Science 364:566-570. https://doi.org/10.1126/science.aav2572

Ross MO, Rosenzweig AC (2017) A tale of two methane monooxygenases. J Biol Inorg Chem 22:307-319. https://doi.org/10.1007/s00775-016-1419-y

Sakai Y, Saiganji A, Yurimoto H, Takabe K, Saiki H, Kato N (1996) The absence of Pmp47, a putative yeast peroxisomal transporter, causes a defect in transport and folding of a specific matrix enzyme. J Cell Biol 134:37-51.

Sakai Y, Yoshida H, Yurimoto H, Yoshida N, Fukuya H, Takabe K, Kato N (1999) Production of fungal fructosyl amino acid oxidase useful for diabetic diagnosis in the peroxisome of *Candida boidinii*. FEBS Lett 459:233-237. https://doi.org/10.1016/S0014-5793(99)01245-4

Schrader J, Schilling M, Holtmann D, Sell D, Filho MV, Marx A, Vorholt JA (2009) Methanol-based industrial biotechnology: current status and future perspectives of methylotrophic bacteria. Trends Biotechnol 27:107-115. https://doi.org/10.1016/j.tibtech.2008.10.009

Sears IB, O'Connor J, Rossanese OW, Glick BS (1998) A versatile set of vectors for constitutive and regulated gene expression in *Pichia pastoris*. Yeast 14:783-790. https://doi.org/10.1002/(SICI)1097-0061(19980615)14:8<783::AID-YEA272>3.0.CO;2-Y

Shiemke AK, Cook SA, Miley T, Singleton P (1995) Detergent solubilization of membrane-bound methane monooxygenase requires plastoquinol analogs as electron donors. Arch Biochem Biophys 321:421-428. https://doi.org/10.1006/abbi.1995.1413

Sirajuddin S, Rosenzweig AC (2015) Enzymatic oxidation of methane. Biochemistry 54:2283-2294. https://doi.org/10.1021/acs.biochem.5b00198

Stewart MQ, Esposito RD, Gowani J, Goodman JM (2001) Alcohol oxidase and dihydroxyacetone synthase, the abundant peroxisomal proteins of methylotrophic

yeasts, assemble in different cellular compartments. J Cell Sci 114:2863-2868.

Tamura N, Oku M, Sakai Y (2010) Atg8 regulates vacuolar membrane dynamics in a lipidation-independent manner in *Pichia pastoris*. J Cell Sci 123:4107-4116. https://doi.org/10.1242/jcs.070045

Trotsenko YA, Torgonskaya ML (2018) Current trends in methylotrophy-based biotechnology. Adv Biotechnol Microbiol 9:555763. https://doi.org/10.19080/AIBM.2018.09.555763

Tschopp JF, Brust PF, Cregg JM, Stillman CA, Gingeras TR (1987) Expression of the *lacZ* gene from two methanol-regulated promoters in *Pichia pastoris*. Nucleic Acids Research 15:3859-3876. https://doi.org/10.1093/nar/15.9.3859

Tuyishime P, Wang Y, Fan L, Zhang Q, Li Q, Zheng P, Sun J, Ma Y (2018) Engineering *Corynebacterium glutamicum* for methanol-dependent growth and glutamate production. Metab Eng 49:220-231. https://doi.org/10.1016/j.ymben.2018.07.011

Vogl T, Sturmberger L, Kickenweiz T, Wasmayer R, Schmid C, Hatzl A-M, Gerstmann MA, Pitzer J, Wagner M, Thallinger GG, Geier M, Glieder A (2016) A toolbox of diverse promoters related to methanol utilization: functionally verified parts for heterologous pathway expression in *Pichia pastoris*. ACS Synth Biol 5:172-186. https://doi.org/10.1021/acssynbio.5b00199

Wen G, Wen X, Shuang S, Choi MMF (2014) Whole-cell biosensor for determination of methanol. Sens Actuators, B 201:586-591. https://doi.org/10.1016/j.snb.2014.04.107

Weston LA, Kadner RJ (1988) Role of *uhp* genes in expression of the *Escherichia coli* sugar-phosphate transport system. J Bacteriol 170:3375-3383. https://doi.org/10.1128/jb.170.8.3375-3383.1988

Witthoff S, Schmitz K, Niedenführ S, Nöh K, Noack S, Bott M, Marienhagen J (2015) Metabolic engineering of *Corynebacterium glutamicum* for methanol metabolism. Appl Environ Microbiol 81:2215. https://doi.org/10.1128/AEM.03110-14

Woolston BM, King JR, Reiter M, Van Hove B, Stephanopoulos G (2018) Improving formaldehyde consumption drives methanol assimilation in engineered *E. coli*. Nat Commun 9:2387. https://doi.org/10.1038/s41467-018-04795-4

Woolston BM, Roth T, Kohale I, Liu DR, Stephanopoulos G (2017) Development of a formaldehyde biosensor with application to synthetic methylotrophy. Biotechnol Bioeng 115:206-215. https://doi.org/10.1002/bit.26455

Wu S, Letchworth GJ (2004) High efficiency transformation by electroporation of *Pichia pastoris* pretreated with lithium acetate and dithiothreitol. Biotechniques 36:152-154. https://doi.org/10.2144/04361DD02

Yurimoto H, Hirai R, Yasueda H, Mitsui R, Sakai Y, Kato N (2002) The ribulose monophosphate pathway operon encoding formaldehyde fixation in a thermotolerant methylotroph, *Bacillus brevis* S1. FEMS Microbiol Lett 214:189-193. https://doi.org/10.1111/j.1574-6968.2002.tb11345.x

Yurimoto H, Komeda T, Lim CR, Nakagawa T, Kondo K, Kato N, Sakai Y (2000) Regulation and evaluation of five methanol-inducible promoters in the methylotrophic yeast *Candida boidinii*. Biochim Biophys Acta 1493:56-63. https://doi.org/10.1016/S0167-4781(00)00157-3

Yurimoto H, Oku M, Sakai Y (2011) Yeast methylotrophy: metabolism, gene regulation and peroxisome homeostasis. Int J Microbiol 2011:101298. https://doi.org/10.1155/2011/101298

Zahn JA, DiSpirito AA (1996) Membrane-associated methane monooxygenase from *Methylococcus capsulatus* (Bath). J Bacteriol 178:1018-1029. https://doi.org/10.1128/jb.178.4.1018-1029.1996

Acknowledgements

First of all, I wish to express my deepest gratitude to Professor Yasuyoshi Sakai, Division of Applied Life Sciences, Graduate School of Agriculture, Kyoto University, for his directions and valuable discussion during the entire course of this work. His ideas/thoughts always stimulated my scientific interests and enhanced my ability of logical thinking.

I would like to show my great appreciation to Associate Professor Hiroya Yurimoto, Division of Applied Life Sciences, Graduate School of Agriculture, Kyoto University, for his invaluable support and direct supervisions from the initial to the final stages of this research work. He had always given me appropriate advice which I could rely on.

I am indebted to Specially Appointed Associate Professor Jun Hoseki, Research Unit for Physiological Chemistry, Kyoto University, for generously sharing his knowledge and expertise, especially in the field of protein engineering, which formed the basis of this study.

I wish to thank Associate Professor Masahide Oku, Department of Bioscience and Biotechnology, Faculty of Bioenvironmental Science, Kyoto University of Advanced Science, for guiding in the field of yeast genetics and microscopy. He was always there and ready to offer his assistance when I was in trouble.

I would like to extend my thanks to Senior Lecturer Hiroyuki Iguchi, Department of Agriculture and Food Technology, Faculty of Bioenvironmental Science, Kyoto University of Advanced Science, for teaching me a number of vital techniques and procedures, especially in the experiments related to Section II of Chapter II and Chapter III.

I am grateful to my research collaborators, Mr. Kento Fujisawa, Mr. Daisuke Hayashi, Mr. Miyabi Yamakita, Mr. Koji Iwasaki and Mr. Kohei Kida. In addition to the collaborations, they gave me a lot of suggestions, stimulations and encouragements at a variety of stages of this work.

My special thanks are due to Professor Jun Ogawa and Associate Professor Shigenobu Kishino, Division of Applied Life Sciences, Graduate School of Agriculture, Kyoto University, for generous permission of use and technical instruction of GC/MS.

I would like to express my gratitude to the previous and present members of Laboratory of Microbial Biotechnology, Division of Applied Life Sciences, Graduate School of Agriculture, Kyoto University, for their friendship and cooperation throughout this study. Special thanks are due to Ms. Yuri Fujita, Ms. Mitsuko Sugiyama, Ms. Shiori Katayama, Dr. Saori Oda, Dr. Shin Ohsawa, Dr. Kosuke Shiraishi, Dr.Yuki Oku, Dr.Yusuke Yoshida, Mr. Ryota Ikeda, Ms. Yoko Kagohashi, Mr. Tomohiro Kuroita, Ms. Momoko Shibata, Mr. Norima Tsukura and Mr. Susumu Nishida, for exciting discussions, honest passion and warm supports, in both science and private life.

I wish to express my thanks to professors, supervisors and friends of Division of Applied Life Sciences, Graduate School of Agriculture, Kyoto University, and of other communities. Their existence always encouraged me when I hit a wall.

And at the end but not least, I would like to thank my family. They were receptive to my decision to do what I wanted to do, and supported me materially and mentally, throughout my life as a student. I sincerely appreciate it.

Publications

1. **Takeya T**, Yurimoto H, Sakai Y (2018) A *Pichia pastoris* single-cell biosensor for detection of enzymatically produced methanol. Appl Microbiol Biotechnol 102:7017–7027. https://doi.org/10.1007/s00253-018-9144-9

2. **Takeya T**, Yamakita M, Hayashi D, Fujisawa K, Sakai Y, Yurimoto H (2020) Methanol production by reversed methylotrophy constructed in *Escherichia coli*. Biosci Biotechnol Biochem 84: 1062-1068. https://doi.org/10.1080/09168451.2020.1715202

3. **Takeya T**, Kida K, Iwasaki K, Sakai Y, Yurimoto H (Manuscript in preparation) Visualization of cellular methane oxidation activity with a yeast single-cell methanol sensor